

Supporting Information

Molecular Binding Behaviors and Thermodynamics of Ferrocenyl Dimethylaminium Derivatives by Anionic Pillar[5]arene

Cui-Fang Zhang, Sheng-Hua Li, Cai-Cai Zhang, and Yu Liu^{a,b*}

^a *Department of Chemistry, State Key Laboratory of Elemento-Organic Chemistry,
Nankai University, Tianjin 300071, P. R. China*

^b *Collaborative Innovation Center of Chemical Science and Engineering, Nankai
University, Tianjin 300071, P. R. China*

E-mail: yuliu@nankai.edu.cn

Contents

1. General information	3
2. Synthetic procedure	5
3. ^1H NMR, ^{13}C NMR spectra and mass spectra of compound 8, 9, 10 and FC_4	8
4. ^1H NMR spectra of FC_n^+ and FC_4 in the absence and presence of 4C-WP5A	15
5. Job plot of G with 4C-WP5A by ^1H NMR titration.....	20
6. Association constants determination for the complexation for G and 4C-WP5A by ^1H NMR titration	25
7. The investigation of the complexation for FC_{18}^+ and 4C-WP5A.....	33
8. Reference	36

1. General information

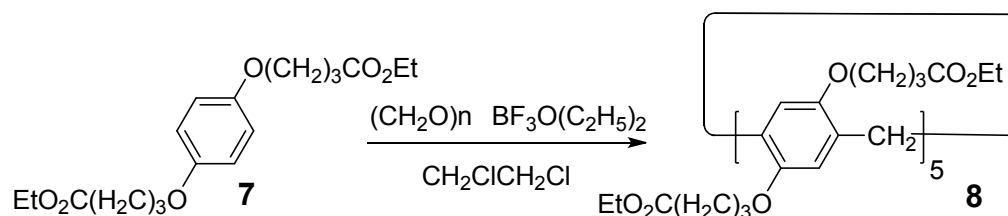
Guest molecules FC_n^+ were synthesized according to the literature procedure^{S1}. The monomer diethyl 4,4'-(1,4-phenylenebis(oxy))dibutanoate (compound **7**) was prepared according to reported procedures^{S2}. Solvents were either employed as purchased or dried according to procedures described in the literature. Column chromatography was performed on silica gel (200–300 mesh). All of experiments were performed at room-temperature unless noted otherwise. ^1H NMR and ^{13}C NMR spectra were recorded on a Bruker AVANCE AV400 (400 MHz and 100 MHz). Signal positions were reported in part per million (ppm) relative to the residual solvent peaks used as an internal standard with the abbreviations s, t, q, and m, denoting singlet, triplet, quartlet and multiplet, respectively. The residual ^1H peak of deuterated solvent appeared at 7.26 ppm in CDCl_3 , at 4.79 ppm in D_2O and at 2.50 ppm in $(\text{CD}_3)_2\text{SO}$, while the ^{13}C peak of CDCl_3 at 77.1 ppm and $(\text{CD}_3)_2\text{SO}$ at 39.5 ppm. All coupling constants J are quoted in Hz. Mass spectra were performed on Varian 7.0TFTICR-MS with MAIDI resource and on an Agilent 6520 Q-TOF LC/MS with ESI ionization.

A thermostatted and fully computer-operated isothermal calorimetry (VP-ITC) instrument was used for all the microcalorimetric experiments. The ITC experiments were performed at 25 °C in aqueous solution, giving the association constants (K_a) and the thermodynamic parameters of guests upon complexations. In each run, a solution of guest in a 0.250 mL syringe was sequentially injected with stirring at 300

rpm into a solution of host in the sample cell (1.4227 mL volume). A control experiment to determine the heat of dilution was carried out for each run by performing the same number of injections with the same concentration of guest compound as used in the titration experiments into a same solution without the host compound. The dilution enthalpies determined in control experiments were subtracted from the enthalpies measured in the titration experiments to obtain the net reaction heat. All thermodynamic parameters reported in this work were obtained by using the “one set of binding sites” model. Two titration experiments were independently performed to give the averaged values with reasonable errors.

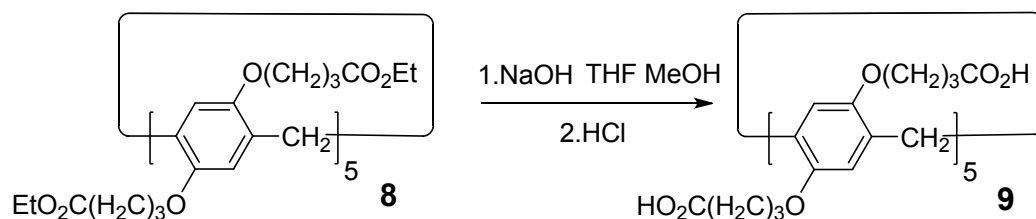
2. Synthetic procedure

a. The synthesis of compound 8



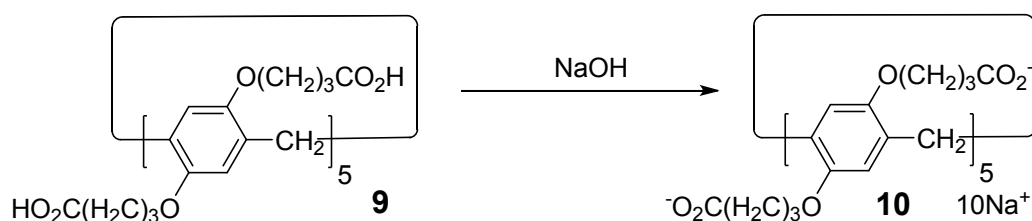
To a solution of compound 7 (676 mg, 2 mmol) in 1,2-dichloroethane (10 mL) was added paraformaldehyde (186 mg, 6 mmol). Then, 0.25 mL (2 mmol) boron trifluoride diethyletherate BF₃·Et₂O was added to the solution, and the mixture was stirred at room temperature for 30 min. Then the mixture was quenched with water and the organic layer was washed with water, saturated aqueous NaHCO₃ solution and brine, dried over Na₂SO₄ and concentrated. The residue was purified by column chromatography on silica gel (petroleum ether /ethyl acetate, 4:1 → 2:1) to get a white powder (490 mg, 70 %). ¹H NMR (400 MHz, CDCl₃, 25 °C) δ: 6.79 (s, 10H), 4.10 (q, 20H, *J* = 8 Hz), 3.90 (m, 20H), 3.72 (s, 10H), 2.57 (t, 20H, *J* = 8 Hz), 2.09–2.15 (m, 20H), 1.17(t, 30H, *J* = 8 Hz). ¹³C NMR (100 MHz, CDCl₃, 25 °C) δ: 170.6, 147.2, 125.8, 112.4, 65.1, 57.9, 28.8, 26.8, 22.7, 11.6. MALDI-FTMS for C₉₅H₁₃₀O₃₀: calcd. [M + Na]⁺: 1773.8542, found: 1773.8542.

b. The synthesis of compound 9



NaOH (334 mg, 8.34 mmol) was dissolved in the 10 mL deionized water. Then aqueous NaOH solution was added to a solution of compound **8** (731 mg, 0.42 mmol) dissolved in the 10 mL THF : MeOH = 1:1. After stirred for 6 h at room temperature, the reaction mixture was concentrated and the residue was acidified with 1M HCl. The white precipitate was collected by filtration, washed with H₂O for several times, dried under vacuum to obtain the compound **9** of corresponding acid. Yield: 580 mg, 94%. ¹H NMR (400 MHz, (CD₃)₂SO, 25 °C) δ: 12.18 (s, 10H), 6.83 (s, 10H), 4.07 (s, 10H), 3.83 (s, 10H), 3.67 (s, 10H), 2.51 (s, 20H), 2.02 (s, 20H). ¹³C NMR (400 MHz, (CD₃)₂SO, 25 °C) δ: 174.7, 149.5, 128.3, 114.5, 67.7, 31.1, 29.2, 28.4. MALDI-FTMS for C₇₅H₉₀O₃₀: calcd. [M + Na]⁺: 1493.5413, found: 1493.5412.

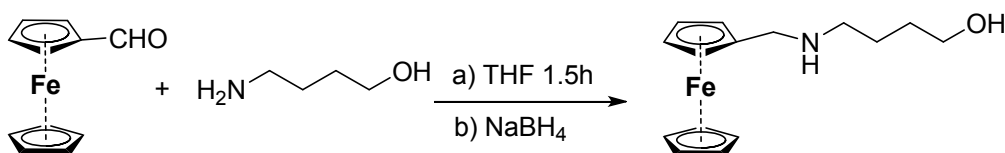
c. The synthesis of compound **10**



198 mg (4.96 mmol) NaOH was added to the suspension of **9** (730 mg, 0.496 mmol) in 100 mL deionized water. After stirred overnight, the solvent was removed under reduced pressure to obtain the **10** (**4C-WP5A**) as white solid. Yield: 814mg, 97%.

Purity: 93% (see Figures S10). ^1H NMR (400 MHz, D_2O , 25 °C) δ : 6.69 (s, 10H), 3.73 (s, 10H), 3.61 (s, 20H), 2.23 (s, 20H), 1.81 (s, 20H). ^{13}C NMR (100 MHz, D_2O , 25 °C) δ : 182.2, 150.1, 129.4, 116.2, 69.3, 34.1, 29.7, 26.0. ESI-HRMS for $\text{C}_{75}\text{H}_{80}\text{O}_{30}$: calcd. $[\text{M}-10\text{Na}+8\text{H}]^{2-}/2$: 734.2679, found: 734.2655.

d. The synthesis of compound FC_4



A mixture of ferrocenecarboxaldehyde (1 mmol, 214.0 mg) and 4-Amino-1-butanol (7 mmol, 623.98 mg) in 20 ml tetrahydrofuran was stirred 1.5 h at room temperature. Then at 0°C added NaBH_4 (10mmol, 380mg) to this mixture. After stirred 1h, the solvent was removed under reduced pressure, a mixture of water (50 mL) and ethyl acetate (50 mL) was added to the crude product. After extraction, the organic layer was dried over Na_2SO_4 and concentrated, then the residue was purified by column chromatography on silica gel (dichloromethane / Methanol, 20:1 \rightarrow 10:1) to get a yellow solid (172 mg, 60 %). ^1H NMR (400 MHz, D_2O , 25 °C) δ : 4.27 (s, 2H), 4.20 (s, 2H), 4.15 (s, 4H), 3.86 (t, 2H, $J = 9.6$ Hz), 3.47 (s, 2H), 2.38 (t, 2H, $J = 10.8$ Hz), 1.52 (m, 2H), 1.45 (m, 2H). ^{13}C NMR (100 MHz, D_2O , 25 °C) δ : 85.6, 68.5, 68.4, 68.0, 62.6, 49.1, 48.5, 32.6, 28.9. MALDI-FTMS for $\text{C}_{15}\text{H}_{21}\text{FeNO}$: calcd. $[\text{M}]^+$: 287.0972, found: 287.0970.

3. ^1H NMR, ^{13}C NMR spectra and mass spectra of compound 8, 9, 10 and FC₄

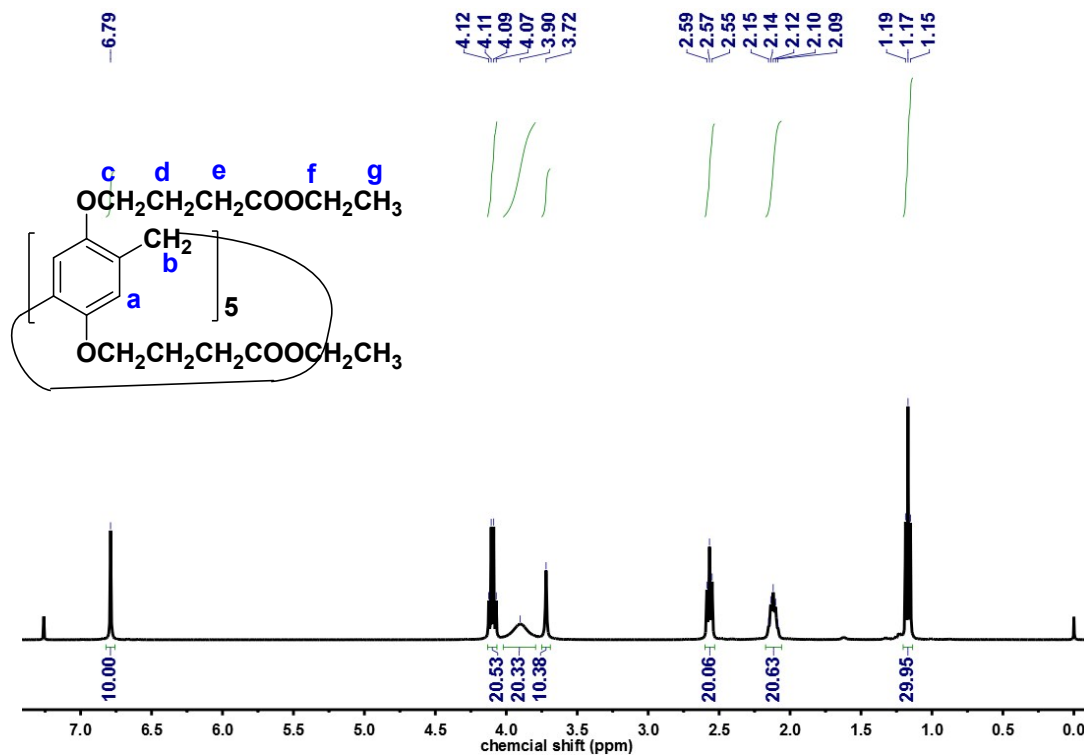


Figure S1. ^1H NMR spectrum (400 MHz, CDCl_3 , 25 °C) of compound 8.

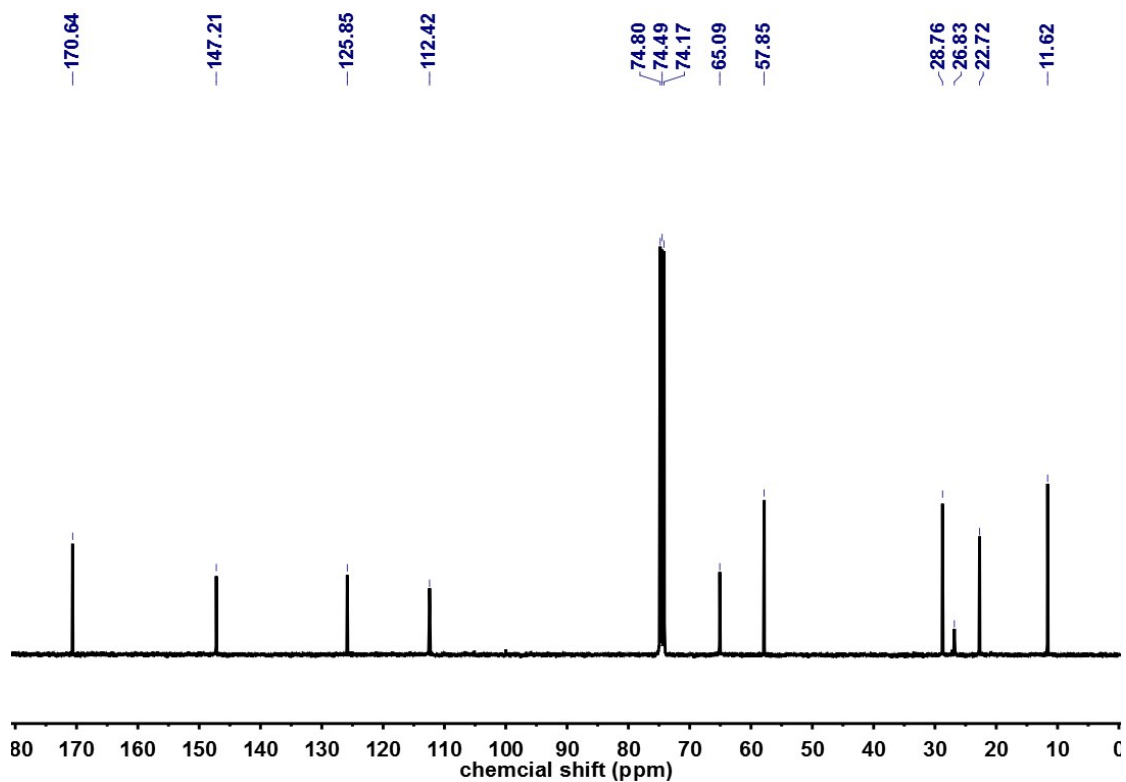


Figure S2. ^{13}C NMR spectrum (100 MHz, CDCl_3 , 25 °C) of compound 8.

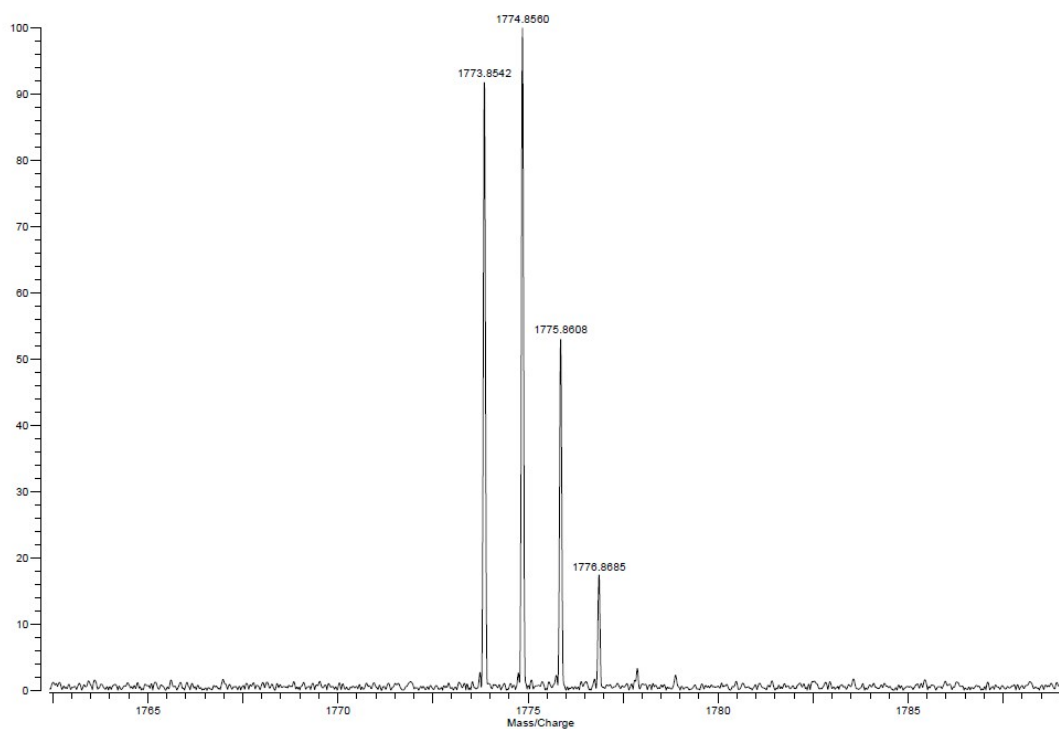


Figure S3. MALDI- FTMS spectrum of compound **8** ($C_{95}H_{130}O_{30}$). The peak at m/z 1773.8542 is assigned to $[M + Na]^+$, calcd.: 1773.8542.

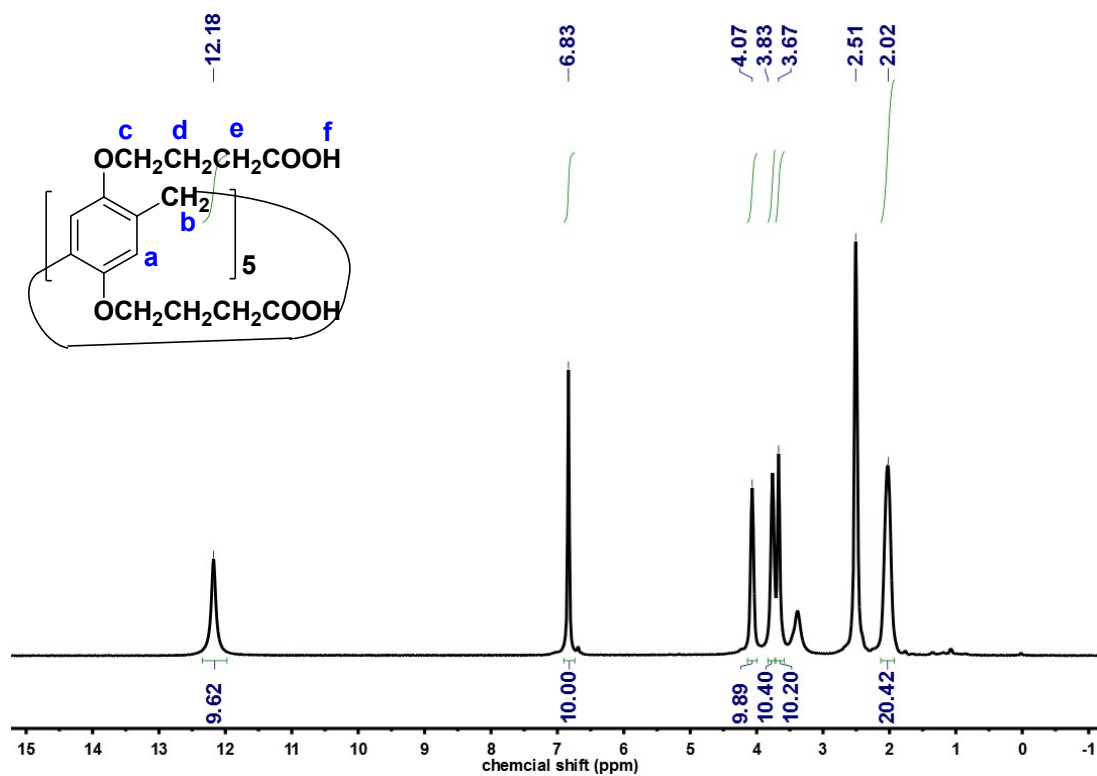


Figure S4. 1H NMR spectrum (400 MHz, $(CD_3)_2SO$, 25 °C) of compound **9**.

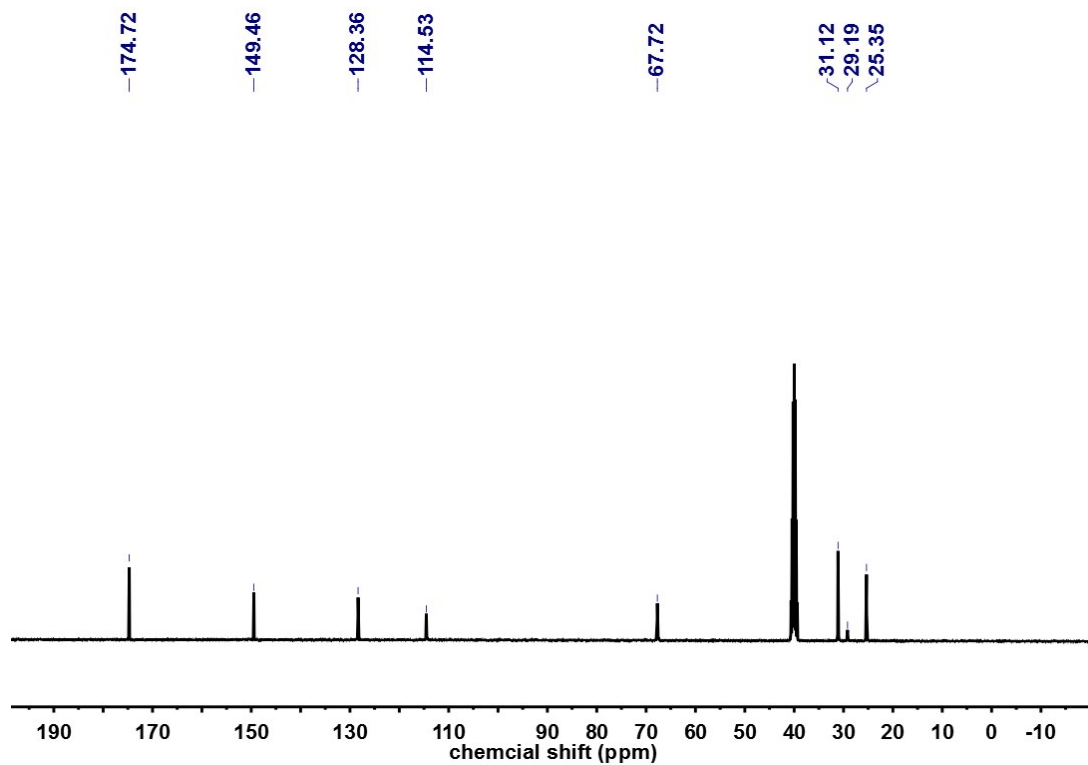


Figure S5. ^{13}C NMR spectrum (100 MHz, $(\text{CD}_3)_2\text{SO}$, 25 °C) of compound **9**.

Varian ProMALDI
File: P5A-COOH_MALDI.trans

Mode: Positive Date: 20-JAN-2015
Scans: 1 Time: 13:50:12
Scale: 34.9809

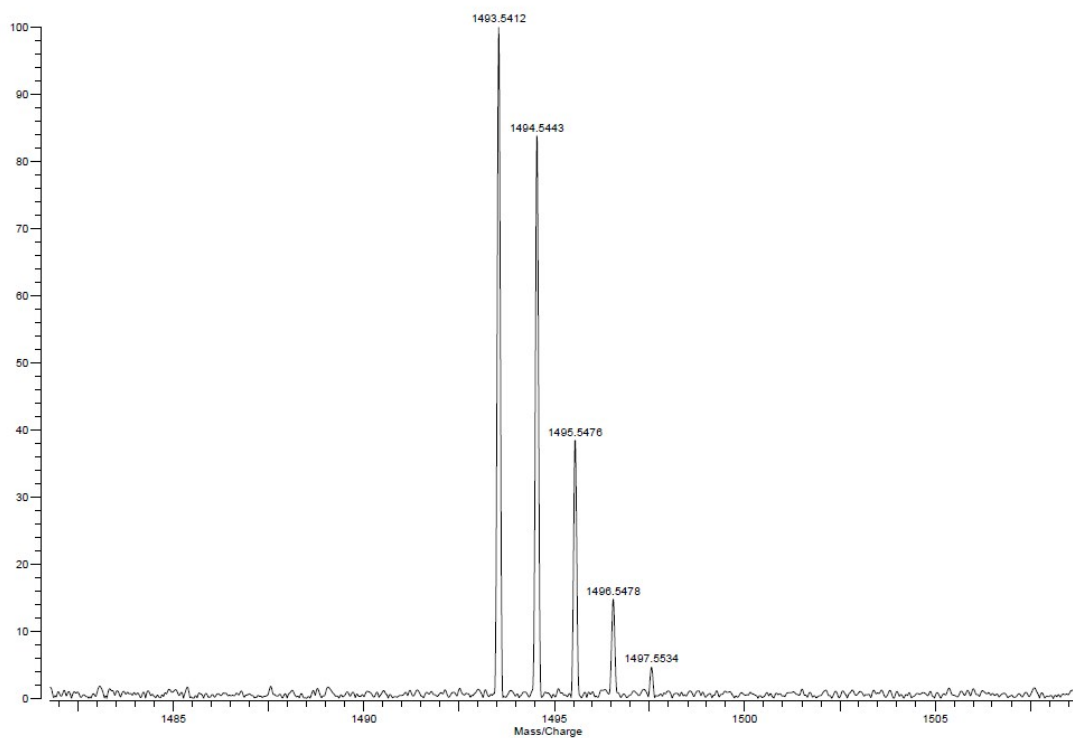


Figure S6. MALDI-FTMS spectrum of compound **9** ($\text{C}_{75}\text{H}_{90}\text{O}_{30}$). The peak at m/z 1493.5412 is assigned to $[\text{M} + \text{Na}]^+$, calcd.: 1493.5413.

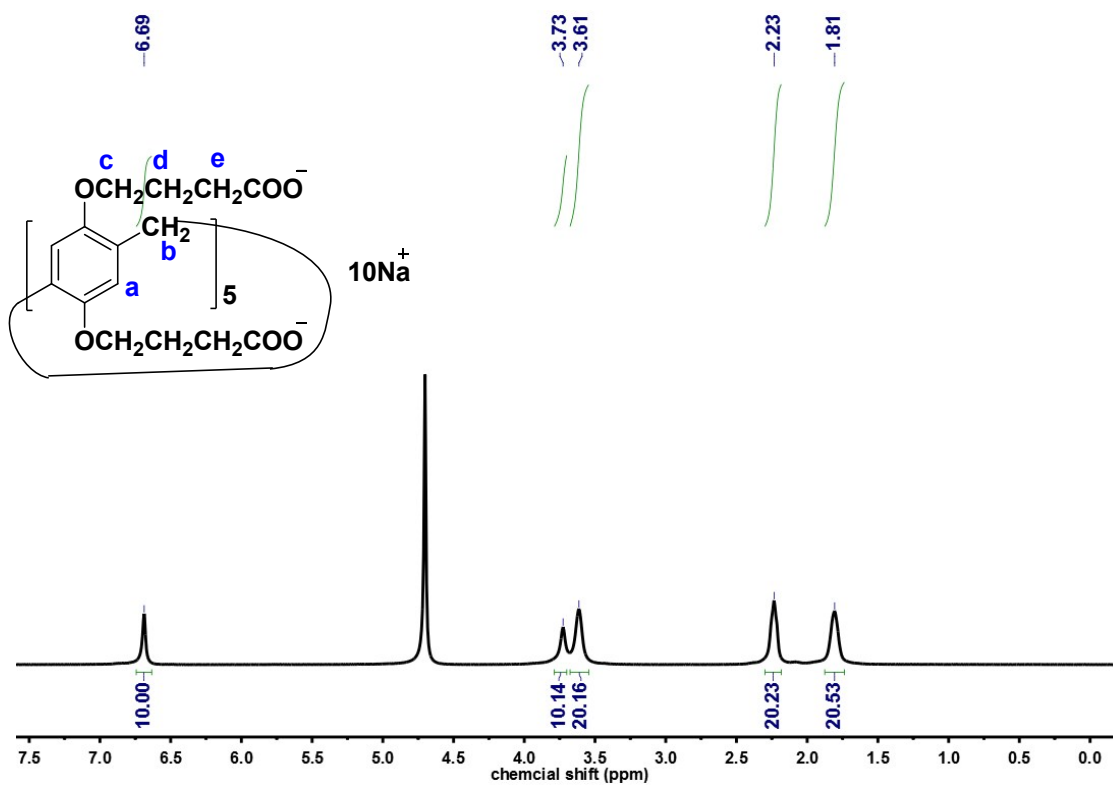


Figure S7. ^1H NMR spectrum (400 MHz, D_2O , 25 $^\circ\text{C}$) of **10**.

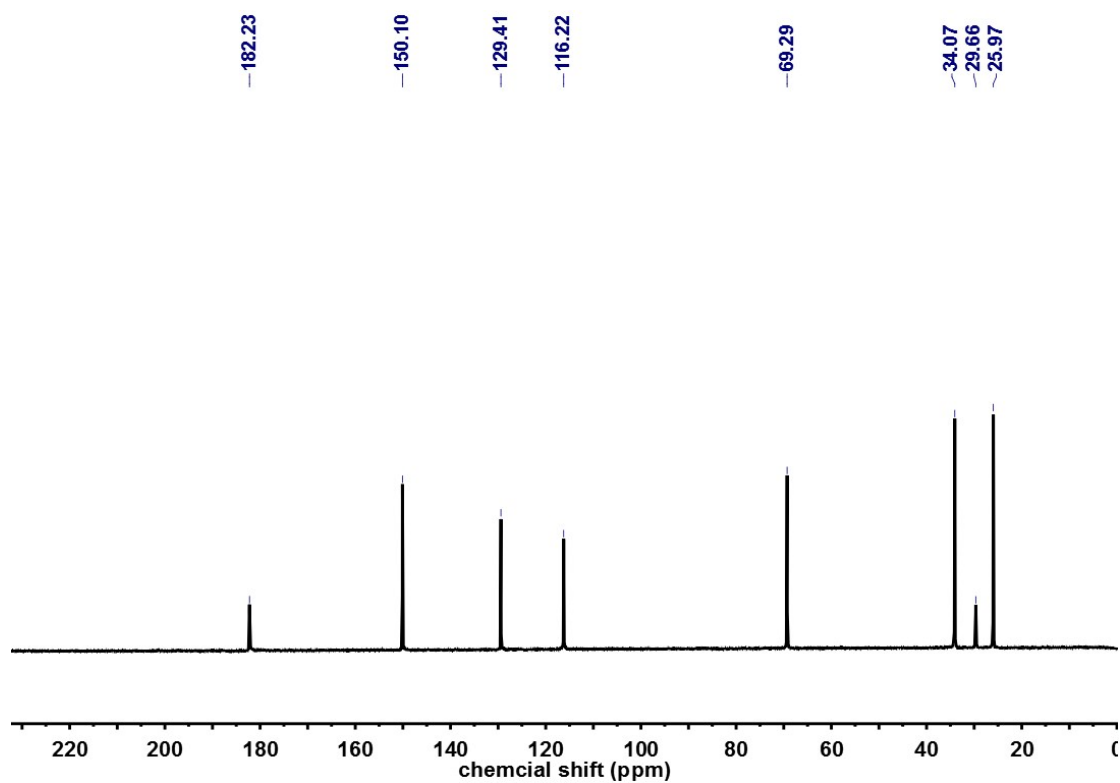


Figure S8. ^{13}C NMR spectrum (100 MHz, D_2O , 25 $^\circ\text{C}$) of **10**.

Sample Name	lc/ms	Position	P1-A1	Instrument Name	Instrument 1	User Name	
Injection Vol	2	InjPosition		Sample Type	Sample	IRM Calibration Status	Some Ions Missed
Data Filename	WP5A-H.d	ACQ Method	chen-ms.m	Comment		Acquired Time	1/30/2015 4:07:30 PM

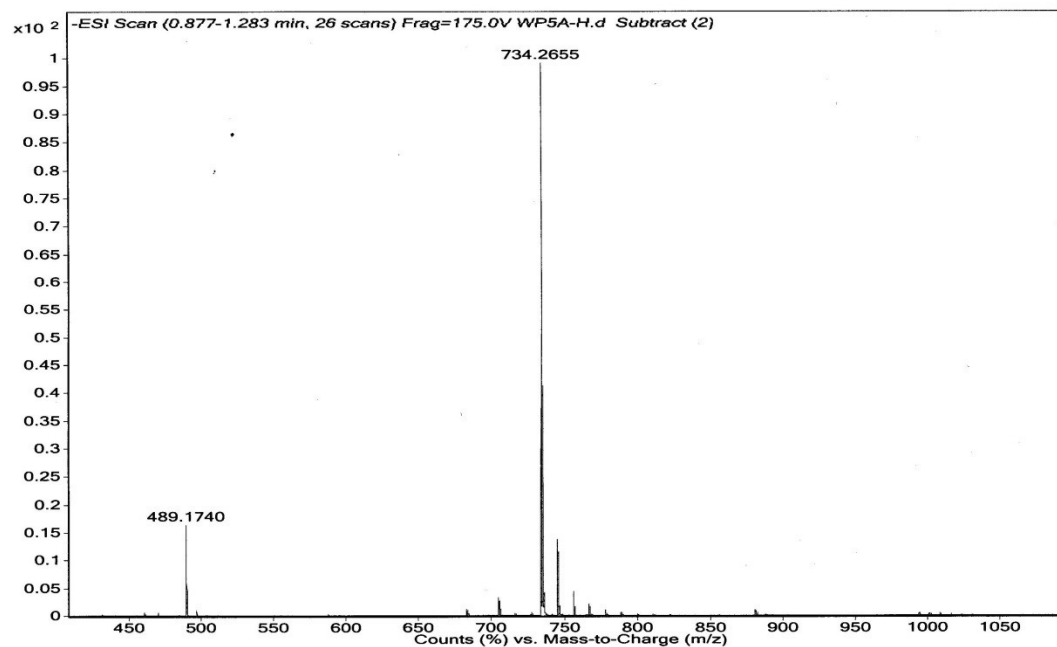


Figure S9. ESI-HRMS spectrum of compound **10** ($C_{75}H_{80}O_{30}$). The peak at m/z 734.2655 is assigned to $[M-10Na + 8H]^{2-}/2$, calcd.: 734.2679.

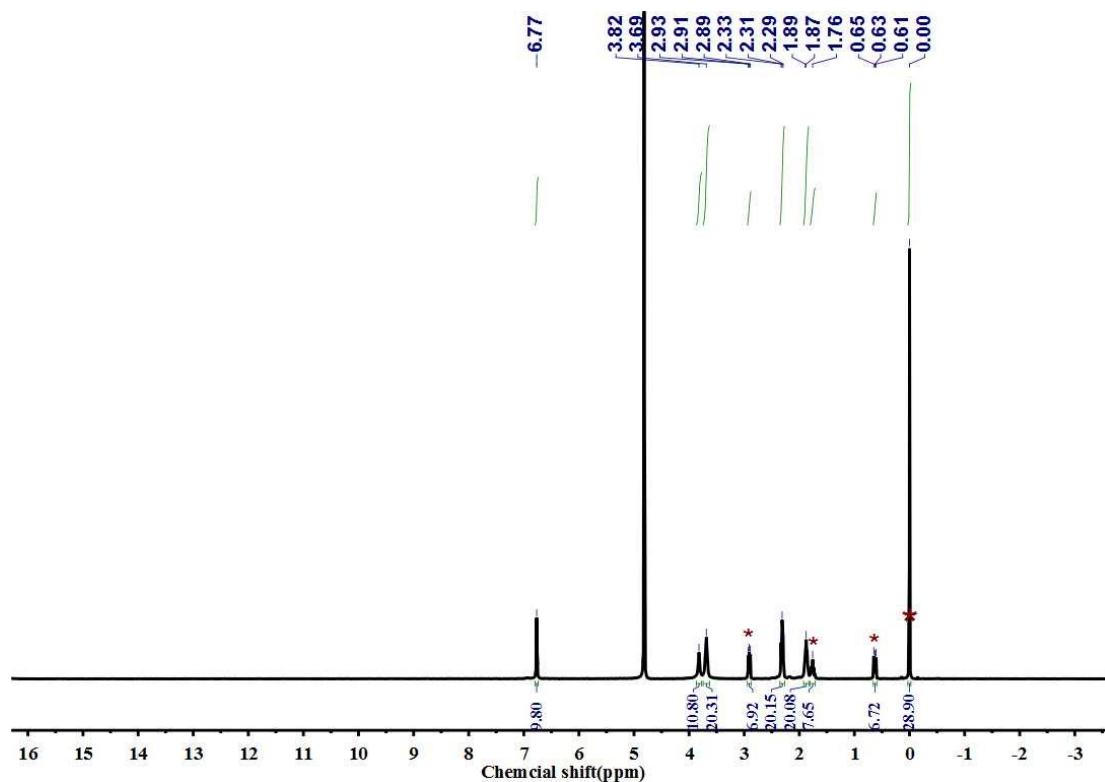


Figure S10. Purity determination of the compound **10** by ^1H NMR spectrum (400 MHz, D_2O , 25 °C) with DSS (3-(trimethylsilyl)-1-propanesulfonic acid sodium salt) as internal standard substance. The (*) express the proton peaks of DSS.

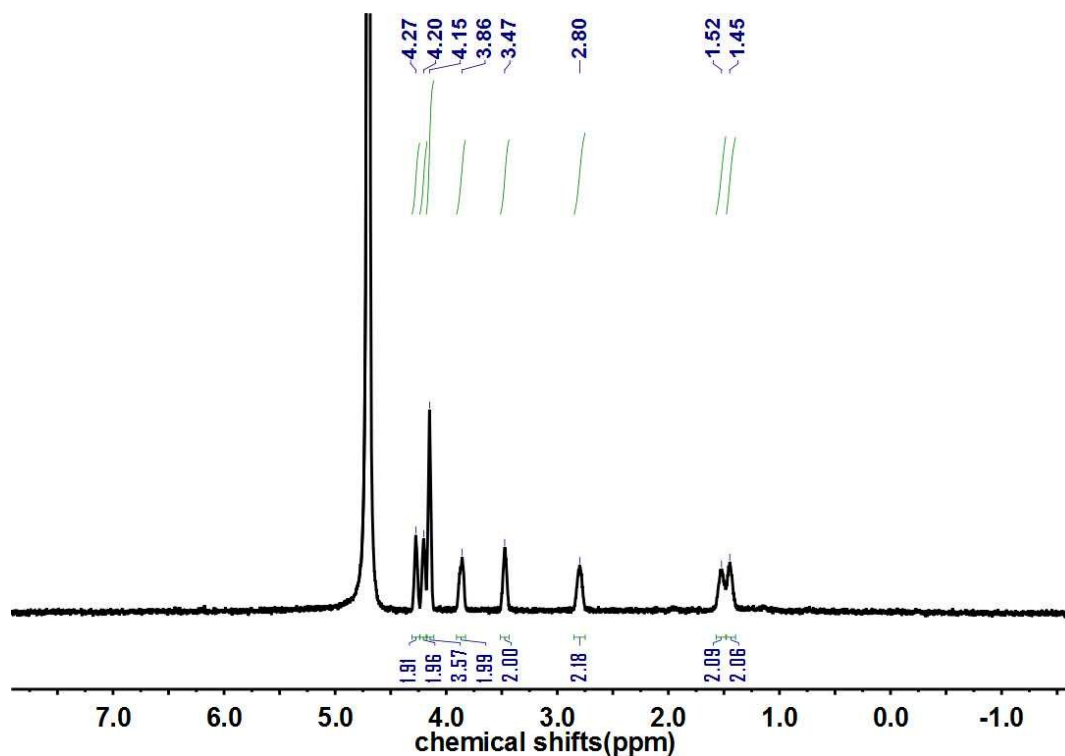


Figure S11. ^1H NMR spectrum (400 MHz, D_2O , 25 °C) of FC_4 .

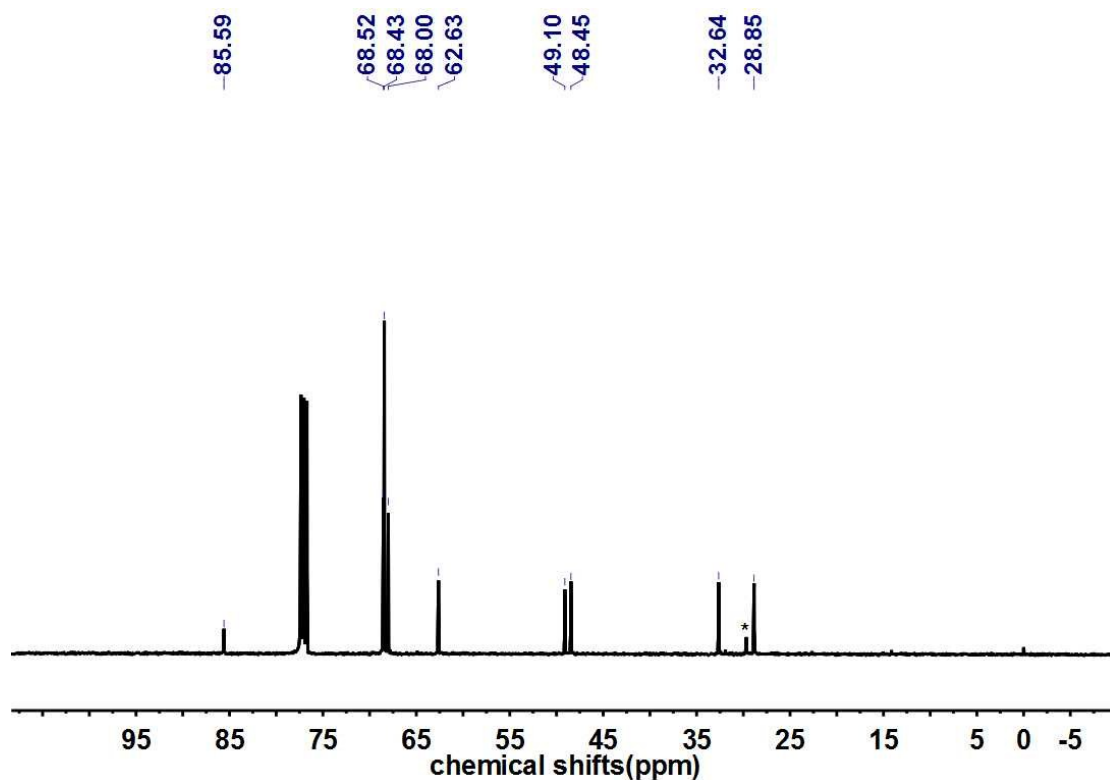


Figure S12. ^{13}C NMR spectrum (100 MHz, CD_3Cl , 25 $^\circ\text{C}$) of FC_4 . The (*) express the carbon peaks of grease.

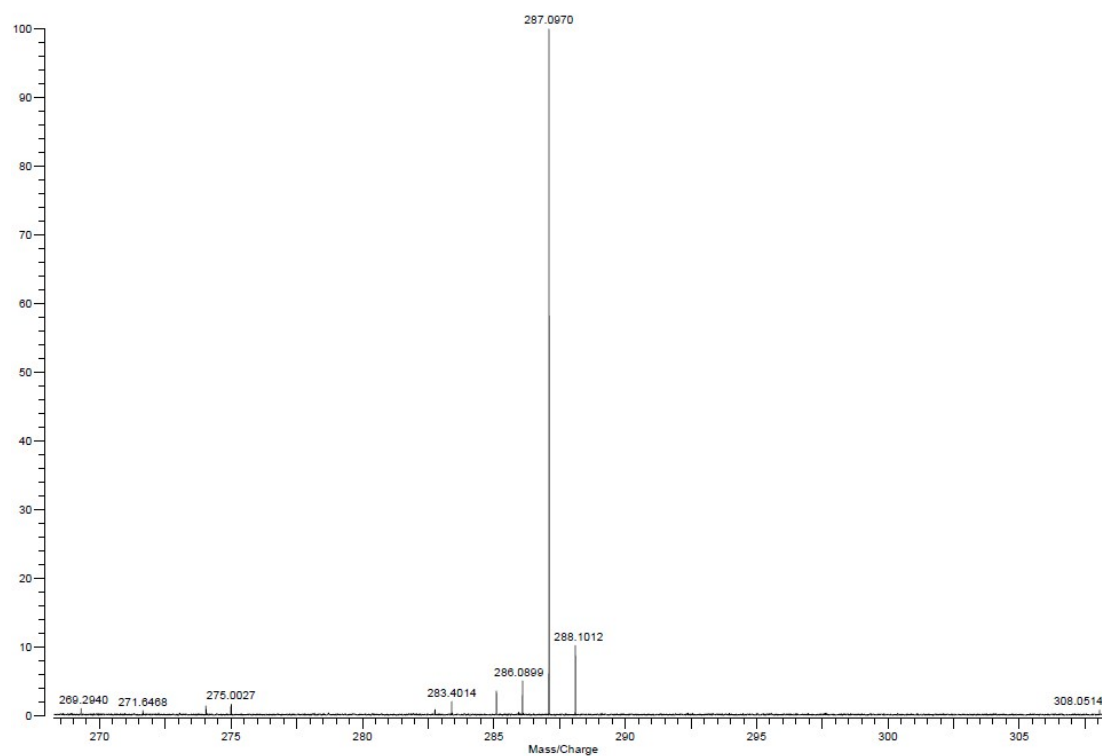


Figure S13. MALDI-FTMS spectrum of compound **FC₄** (C₁₅H₂₁FeNO). The peak at *m/z* 287.0970 is assigned to [M]⁺, calcd.: 287.0972.

4. ¹H NMR spectra of FC_n⁺ and FC₄ in the absence and presence of 4C-WP5A

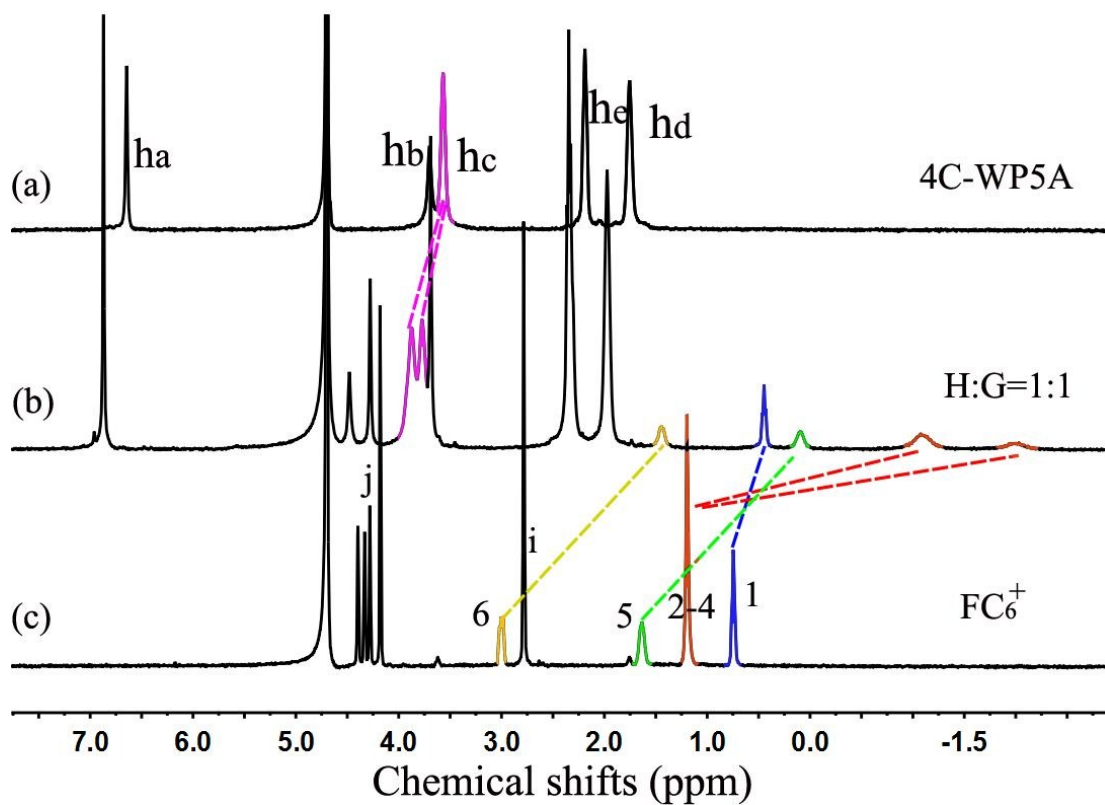


Figure S14. ¹H NMR spectra (D₂O, 293 K, 400 MHz) of (a) 5 mM 4C-WP5A; (b) 5

mM 4C-WP5A + 5 mM FC₆⁺; (c) 5 mM FC₆⁺.

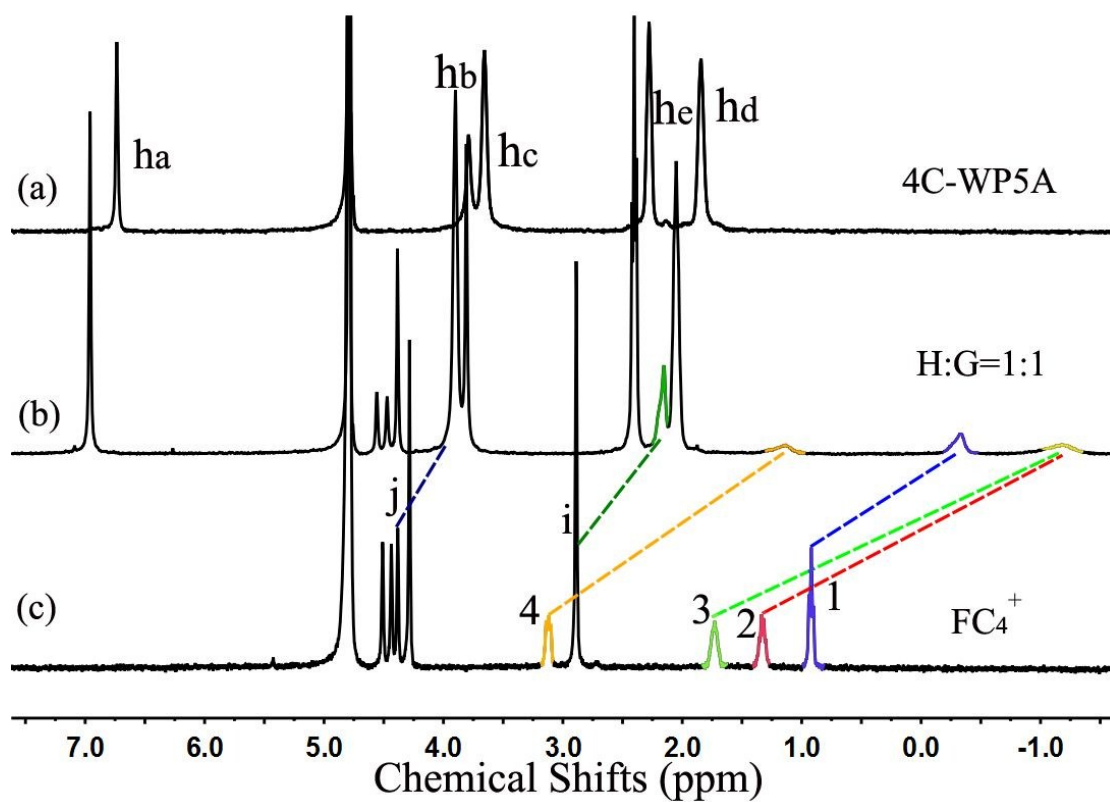


Figure S15. ¹H NMR spectra (D₂O, 293 K, 400 MHz) of (a) 5 mM 4C-WP5A; (b) 5 mM 4C-WP5A + 5 mM FC₄⁺; (c) 5 mM FC₄⁺.

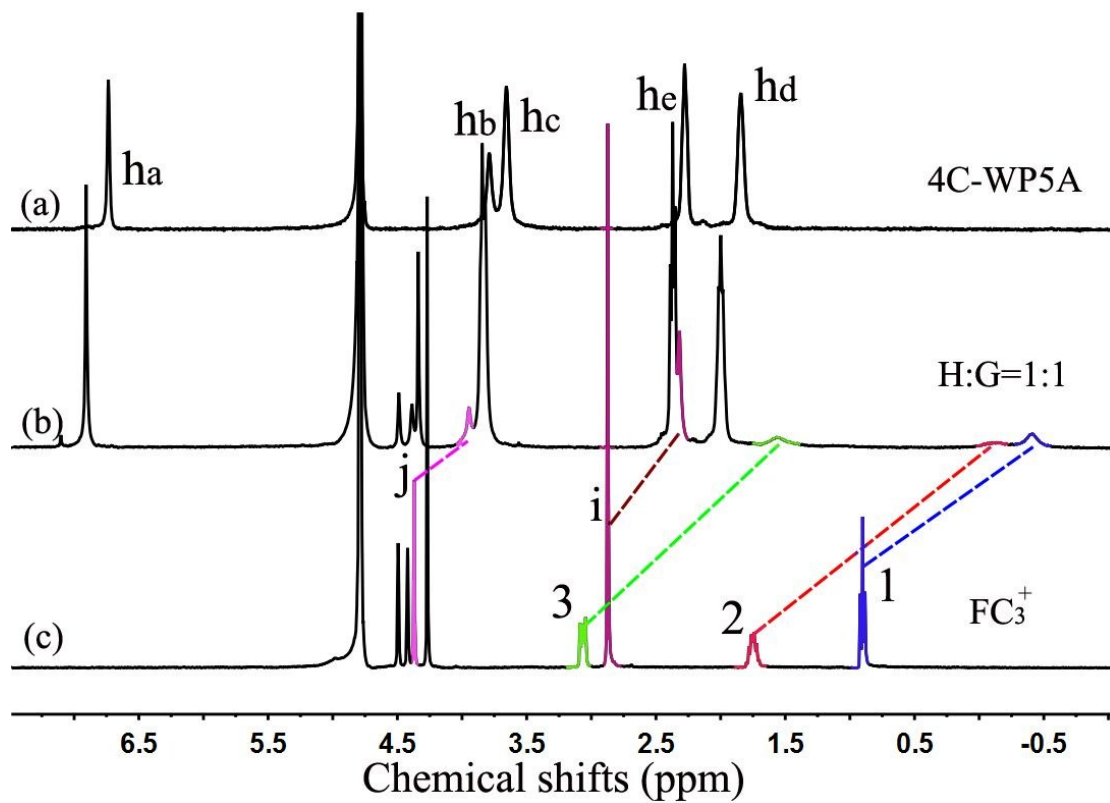


Figure S16. ^1H NMR spectra (D₂O, 293 K, 400 MHz) of (a) 5 mM 4C-WP5A; (b) 5 mM 4C-WP5A + 5 mM FC₃⁺; (c) 5 mM FC₃⁺.

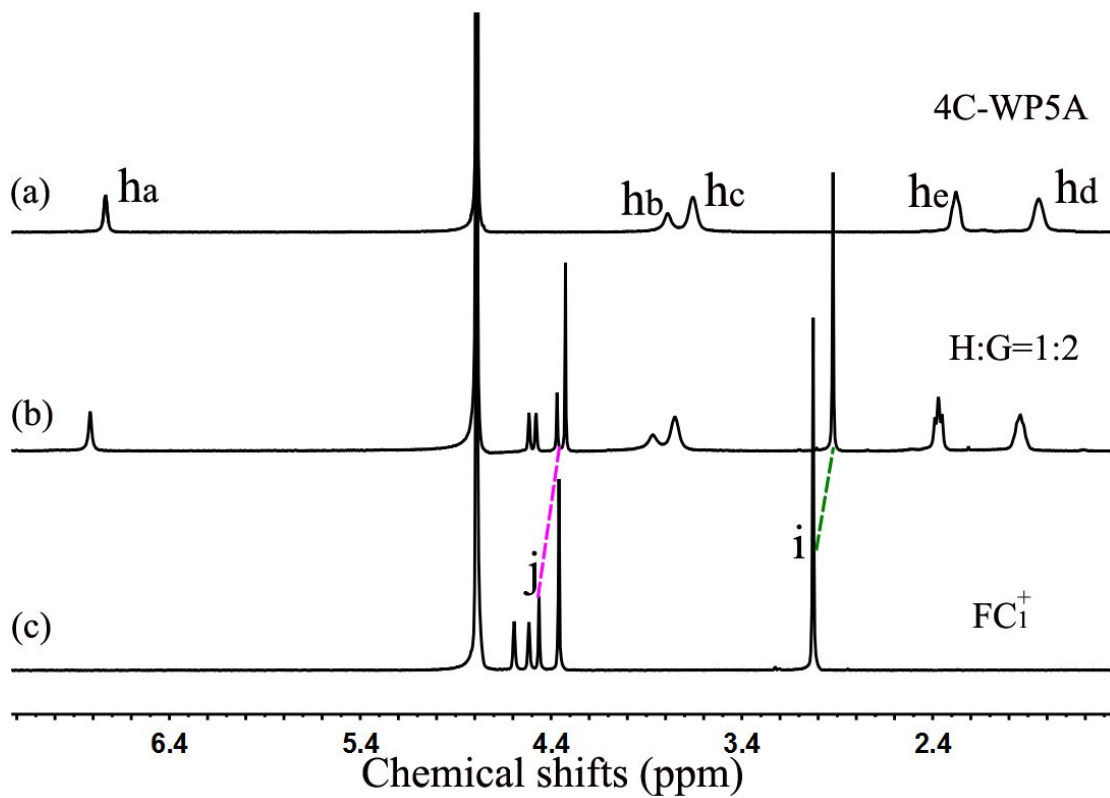


Figure S17. ^1H NMR spectra (D₂O, 293 K, 400 MHz) of (a) 2.5 mM **4C-WP5A**; (b) 2.5 mM **4C-WP5A** + 5 mM **FC₁⁺**; (c) 5 mM **FC₁⁺**.

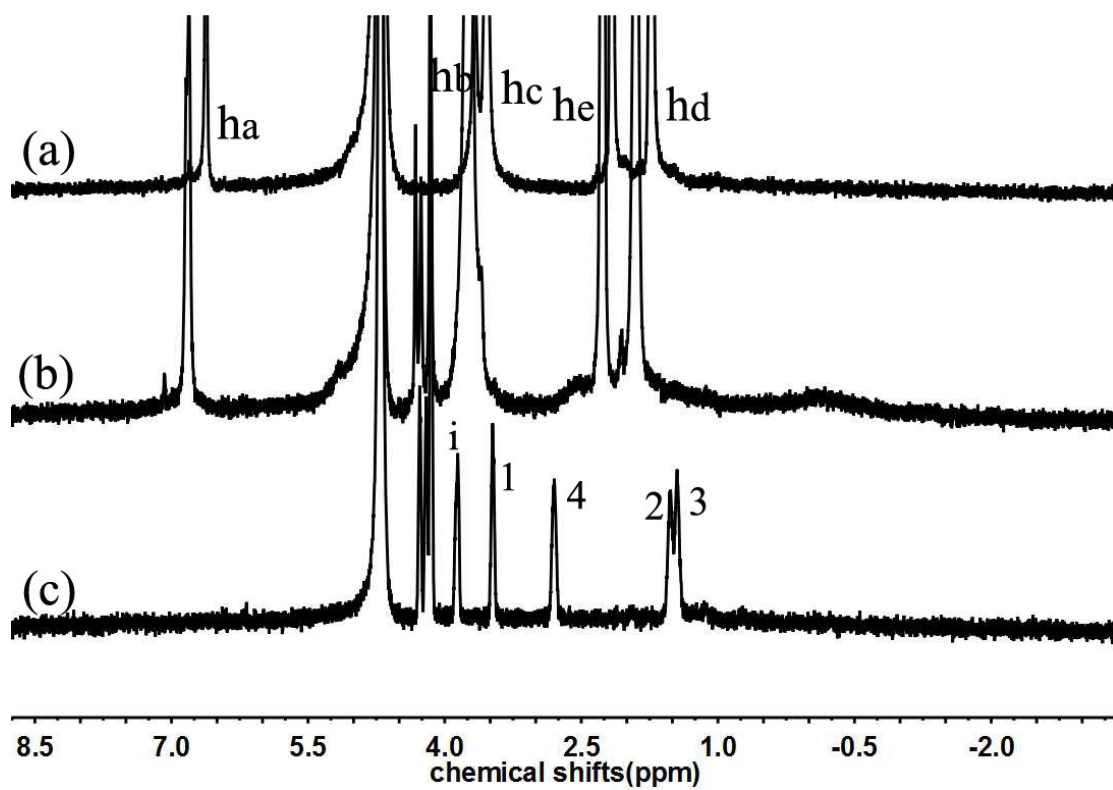


Figure S18. ^1H NMR spectra (D_2O , 293 K, 400 MHz) of (a) 1 mM 4C-WP5A; (b) 1 mM 4C-WP5A + 1 mM FC₄; (c) 1 mM FC₄.

5. Job plot of G with 4C-WP5A by ^1H NMR titration.

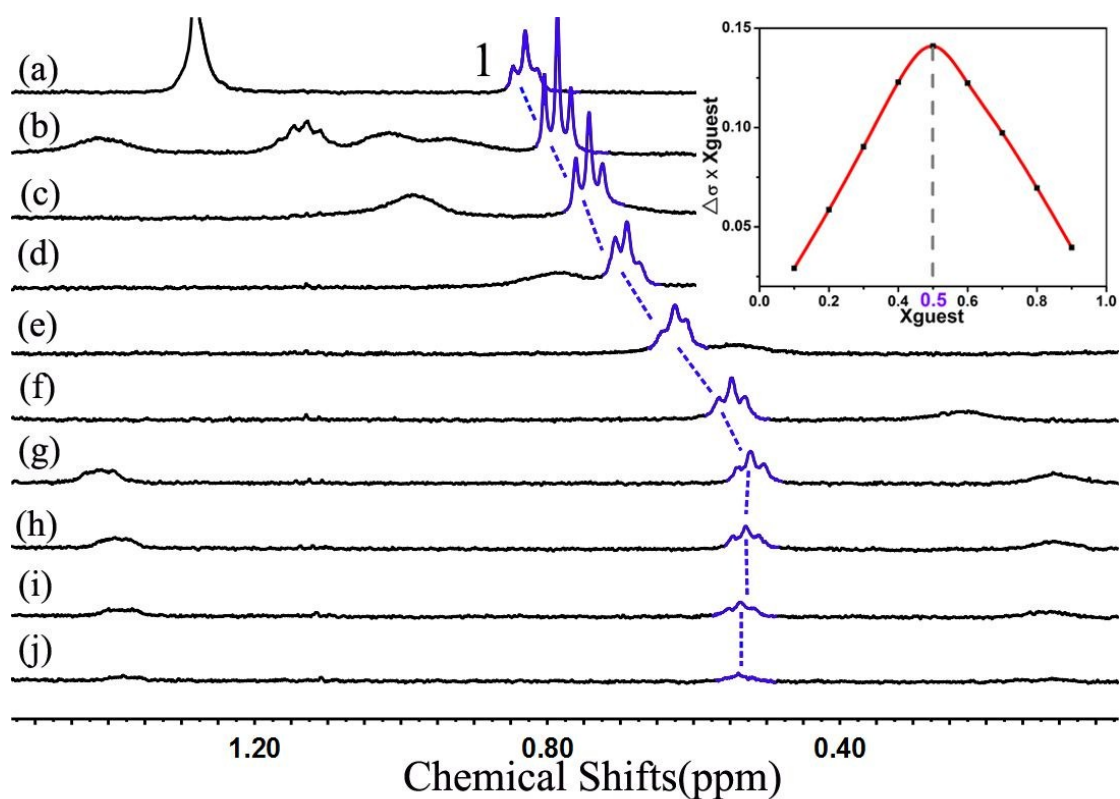


Figure S19. ^1H NMR spectra ($[\text{4C-WP5A}] + [\text{FC}_6^+] = 2.0 \text{ mM}$, D_2O , 298 K, 400 MHz) of the chemical shift changes of H-1 on FC_6^+ with the molar ratio of FC_6^+ is: (a) individual FC_6^+ , (b) 0.90, (c) 0.80, (d) 0.70, (e) 0.60, (f) 0.50, (g) 0.40, (h) 0.30, (i) 0.20, (j) 0.10. Insert: Job plot showing the 1:1 stoichiometry of the complex between **4C-WP5A** and FC_6^+ by ^1H NMR titration.

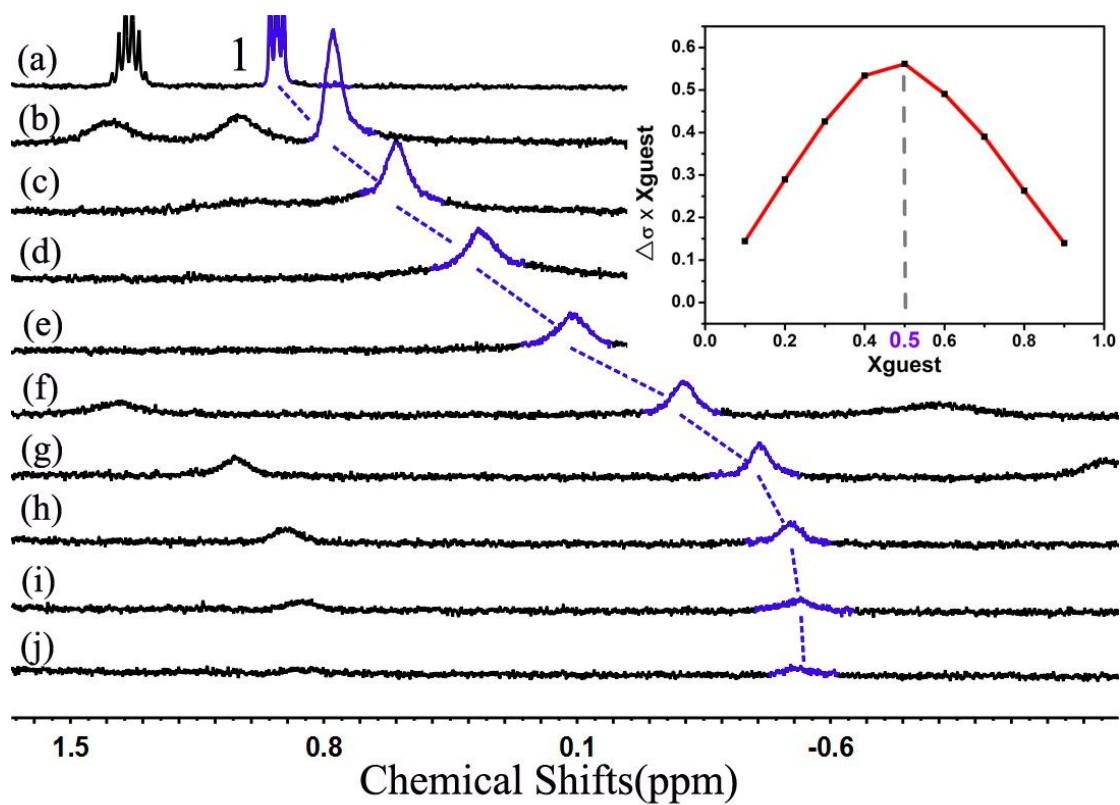


Figure S20. ^1H NMR spectra ($[\text{4C-WP5A}] + [\text{FC}_4^+] = 3.2 \text{ mM}$, D_2O , 298 K, 400 MHz) of the chemical shift changes of H-1 on FC_4^+ with the molar ratio of FC_4^+ is: (a) individual FC_4^+ , (b) 0.90, (c) 0.80, (d) 0.70, (e) 0.60, (f) 0.50, (g) 0.40, (h) 0.30, (i) 0.20, (j) 0.10. Insert: Job plot showing the 1:1 stoichiometry of the complex between **4C-WP5A** and FC_4^+ by ^1H NMR titration.

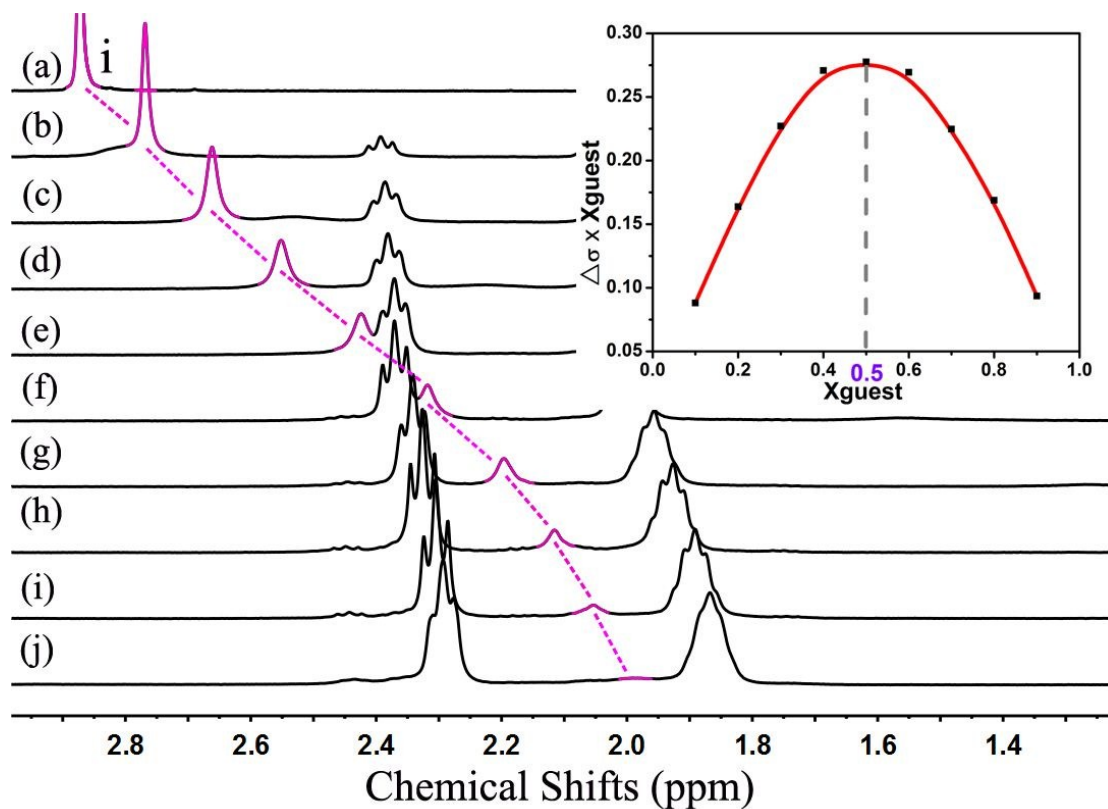


Figure S21. ^1H NMR spectra ($[\text{4C-WP5A}] + [\text{FC}_3^+] = 5 \text{ mM}$, D_2O , 298 K, 400 MHz) of the chemical shift changes of Hi on FC_3^+ with the molar ratio of FC_3^+ is: (a) individual FC_3^+ , (b) 0.90, (c) 0.80, (d) 0.70, (e) 0.60, (f) 0.50, (g) 0.40, (h) 0.30, (i) 0.20, (j) 0.10. Insert: Job plot showing the 1:1 stoichiometry of the complex between **4C-WP5A** and FC_3^+ by ^1H NMR titration.

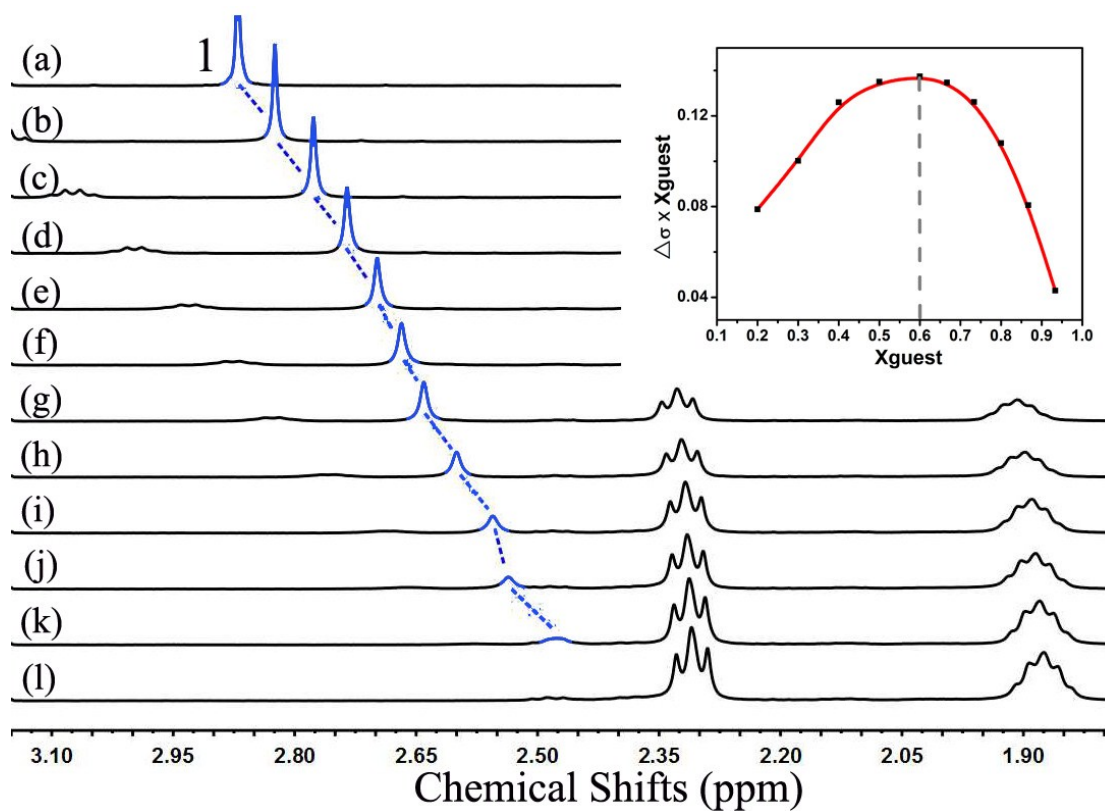


Figure S22. ^1H NMR spectra ($[\mathbf{4C-WP5A}] + [\mathbf{FC}_2^+] = 4.8 \text{ mM}$, D_2O , 298 K, 400 MHz) of the chemical shift changes of H-1 on \mathbf{FC}_2^+ with the molar ratio of \mathbf{FC}_2^+ is: (a) individual \mathbf{FC}_2^+ , (b) 0.93, (c) 0.87, (d) 0.80, (e) 0.73, (f) 0.67, (g) 0.60, (h) 0.50, (i) 0.40, (j) 0.30, (k) 0.20, (l) 0.10. Insert: Job plot showing neither 1:2 nor 1:1 stoichiometry of the complex between $\mathbf{4C-WP5A}$ and \mathbf{FC}_2^+ by ^1H NMR titration.

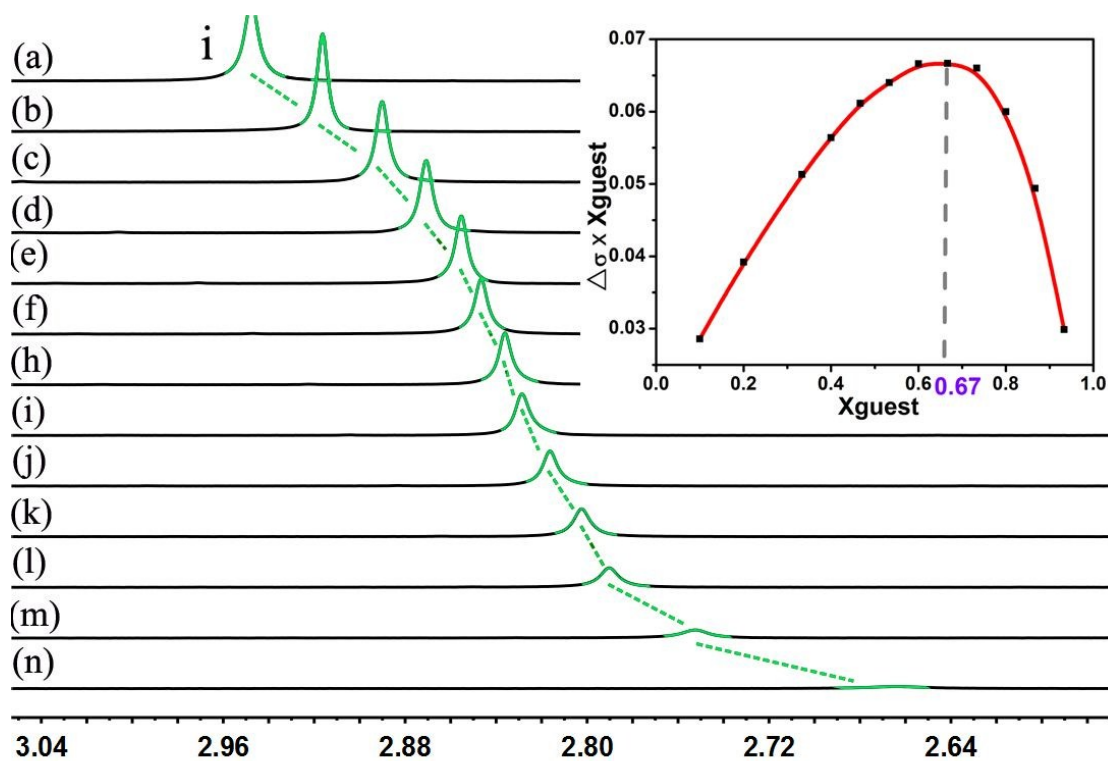


Figure S23. ^1H NMR spectra ($[\mathbf{4C-WP5A}] + [\mathbf{FC}_1^+] = 4.8\text{mM}$, D_2O , 298 K, 400 MHz) of the chemical shift changes of Hi on \mathbf{FC}_1^+ with the molar ratio of \mathbf{FC}_1^+ is: (a) individual \mathbf{FC}_1^+ , (b) 0.93, (c) 0.87, (d) 0.80, (e) 0.73, (f) 0.67, (h) 0.60, (i) 0.53, (j) 0.47, (k) 0.40, (l) 0.33, (m) 0.20, (n) 0.10. Insert: Job plot showing the 1:2 stoichiometry of the complex between $\mathbf{4C-WP5A}$ and \mathbf{FC}_1^+ by ^1H NMR titration.

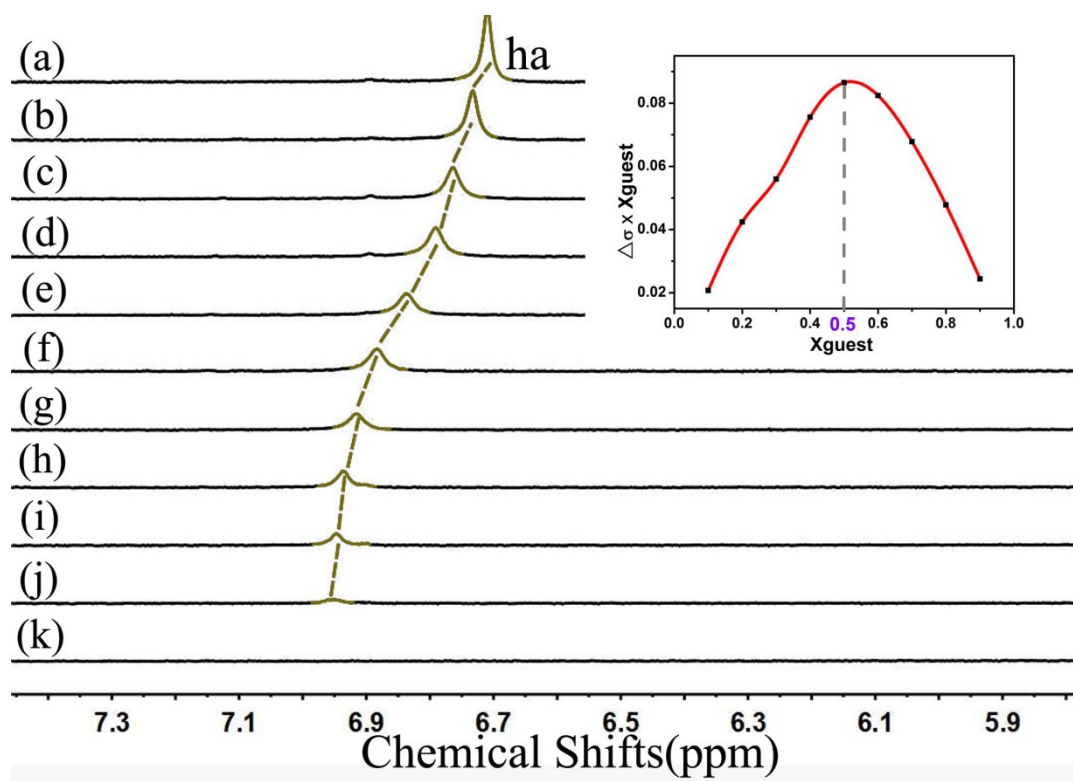


Figure S24. ^1H NMR spectra ($[\mathbf{4C-WP5A}] + [\mathbf{FC}_4] = 1 \text{ mM}$, D_2O , 298 K, 400 MHz) of the chemical shift changes of Ha on $\mathbf{4C-WP5A}$ with the molar ratio of \mathbf{FC}_4 is: (a) individual $\mathbf{4C-WP5A}$, (b) 0.1, (c) 0.20, (d) 0.30, (e) 0.40, (f) 0.50, (g) 0.60, (h) 0.70, (i) 0.80, (j) 0.90, (j) 1.0. Insert: Job plot showing the 1:1 stoichiometry of the complex between $\mathbf{4C-WP5A}$ and \mathbf{FC}_4 by ^1H NMR titration.

6. Association constants determination for the complexation for G and $\mathbf{4C-WP5A}$ by ^1H NMR titration

Association constants of $\mathbf{4C-WP5A} \supset \mathbf{FC}_n^+$ involved were measured by ^1H NMR spectroscopic titrations using a nonlinear curvefitting analysis. The non-linear curvefitting was based on the equation^{S3}:

$\Delta\delta = (\Delta\delta_{\infty}/[G]_0) (0.5[H] + 0.5([G]_0 + 1/Ka) - (0.5([H]^2 + (2[H](1/Ka - [G]_0)) + (1/Ka + [G]_0)^2)^{0.5}))$. Where $\Delta\delta$ is the chemical shift change of proton on G at [H], $\Delta\delta_{\infty}$ is the chemical shift change of proton on G when the guest is completely complex, $[G]_0$ is the fixed initial concentration of the guest, and [H] is the varying concentrations of **4C-WP5A**.

Association constants of **4C-WP5A** \supset **FC₄** involved was also measured by ¹H NMR spectroscopic titrations using a nonlinear curvefitting analysis. The non-linear curve-fitting was based on the equation^{S3}:

$\Delta\delta = (\Delta\delta_{\infty}/[H]_0) (0.5[G] + 0.5([H]_0 + 1/Ka) - (0.5([G]^2 + (2[G](1/Ka - [H]_0)) + (1/Ka + [H]_0)^2)^{0.5}))$. Where $\Delta\delta$ is the chemical shift change of proton on H at [G], $\Delta\delta_{\infty}$ is the chemical shift change of proton on H when the host is completely complex, $[H]_0$ is the fixed initial concentration of the **4C-WP5A**, and [G] is the varying concentrations of **FC₄**.

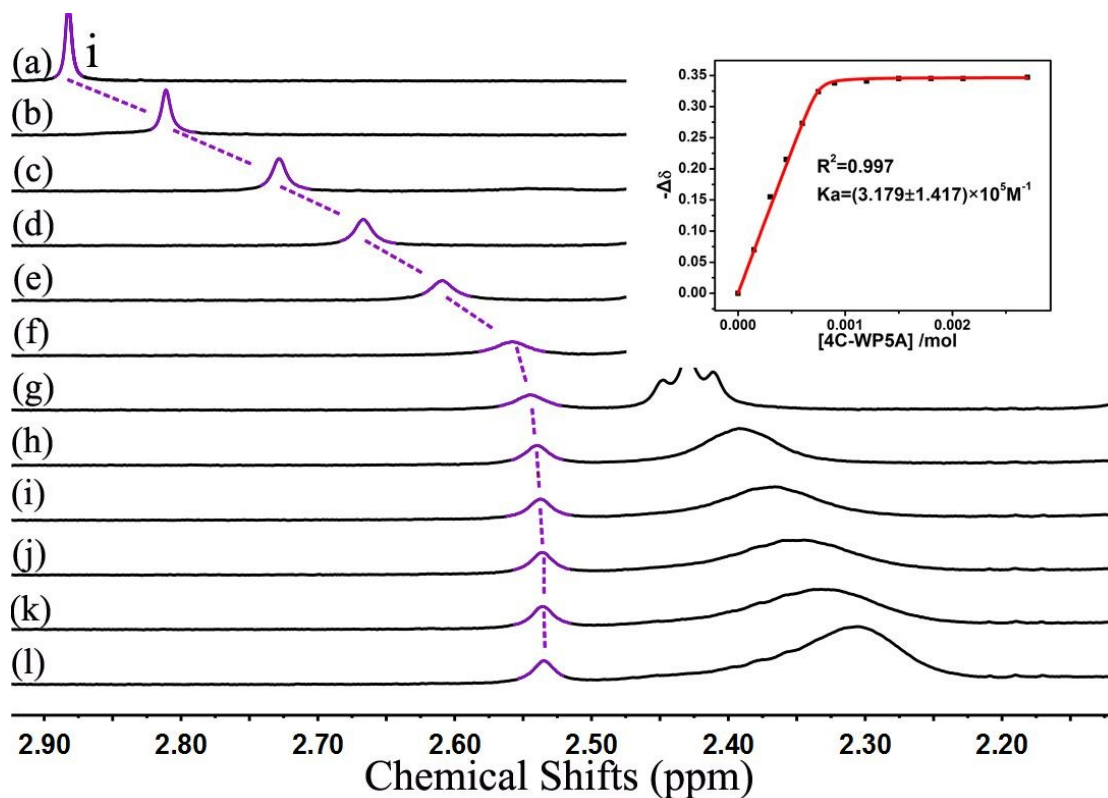


Figure S25. ^1H NMR spectra (D_2O , 293 K, 400 MHz) of FC_8^+ at a concentration of 0.75 mM upon different concentrations of **4C-WP5A**: (a) 0.00 mM, (b) 0.15 mM, (c) 0.30 mM, (d) 0.45mM, (e) 0.60 mM, (f) 0.75 mM, (g) 0.90 mM, (h) 1.20 mM, (i) 1.50 mM, (j) 1.80 mM, (k) 2.10 mM, (l) 2.70 mM. Insert: The chemical shift changes of Hi on FC_8^+ upon addition of **4C-WP5A**. The red solid line was obtained from the non-linear curve-fitting.

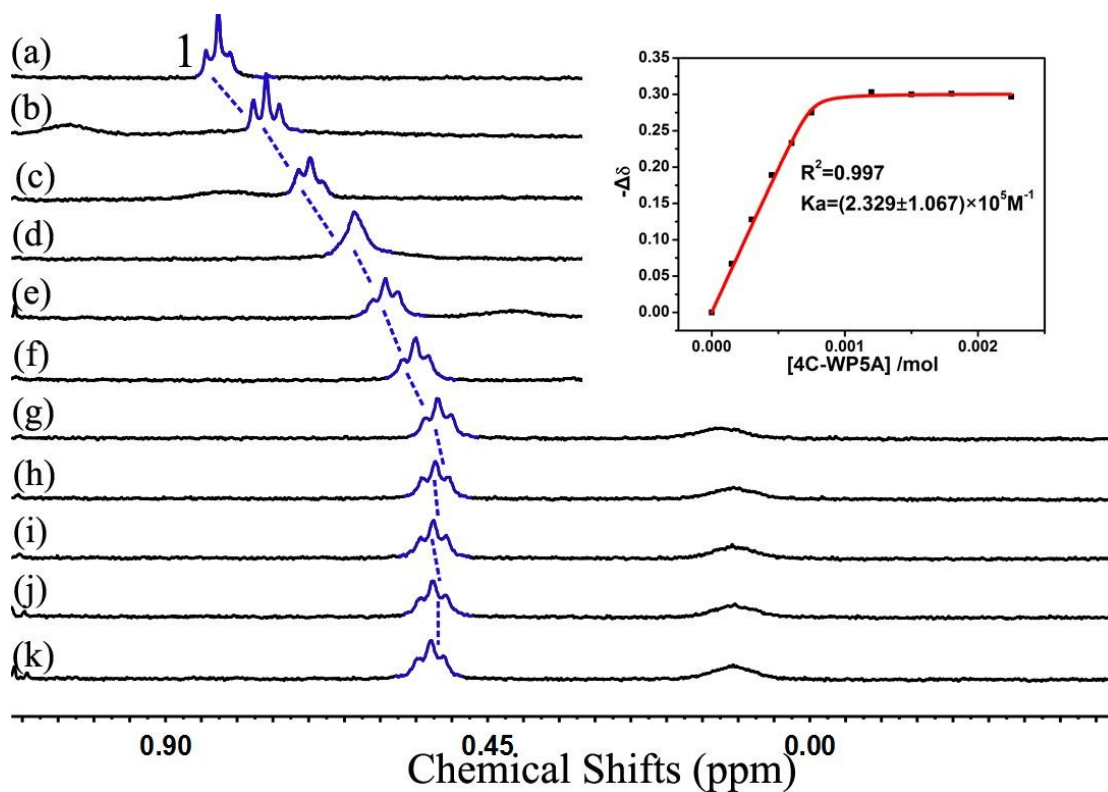


Figure S26. ¹H NMR spectra (D₂O, 293 K, 400 MHz) of at FC₆⁺ a concentration of 0.75 mM upon different concentrations of 4C-WP5A: (a) 0.00 mM, (b) 0.15 mM, (c) 0.30 mM, (d) 0.45 mM, (e) 0.60 mM, (f) 0.75 mM, (g) 0.90 mM, (h) 1.20 mM, (i) 1.50 mM, (j) 1.80 mM, (k) 2.25 mM. Insert: The chemical shift changes of H-1 on FC₆⁺ upon addition of 4C-WP5A. The red solid line was obtained from the non-linear curve-fitting.

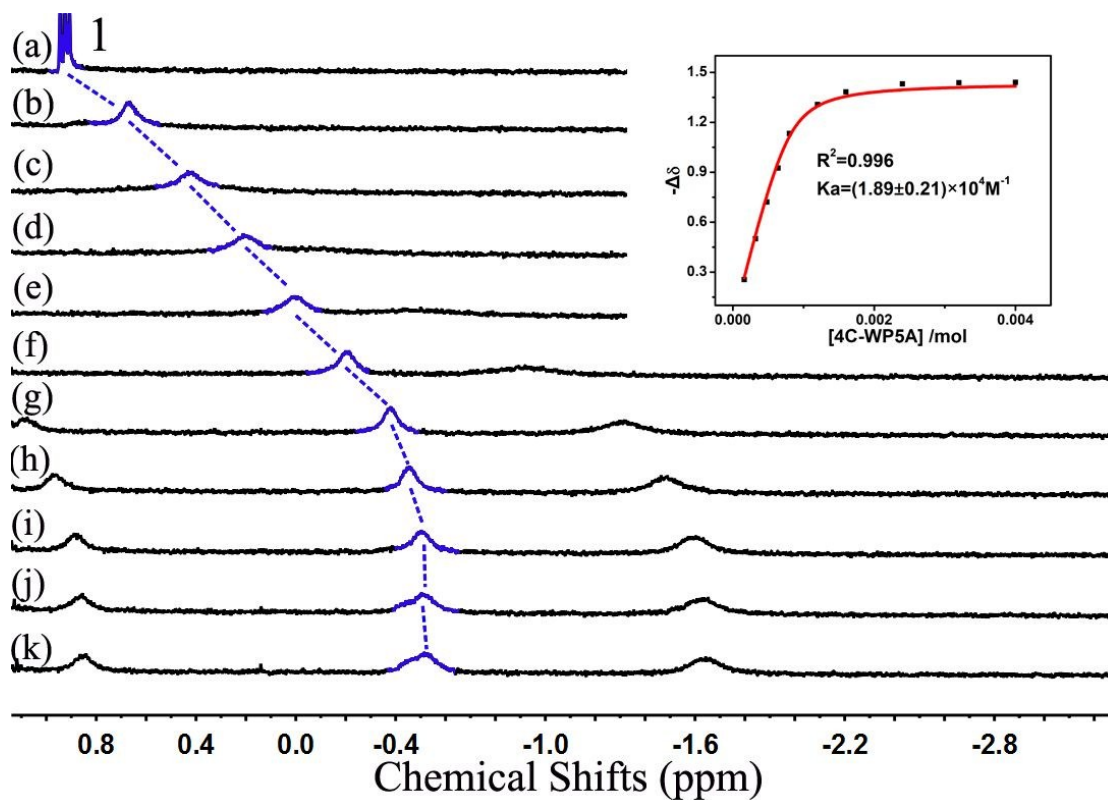


Figure S27. ^1H NMR spectra (D_2O , 293 K, 400 MHz) of FC_4^+ at a concentration of 0.8 mM upon different concentrations of **4C-WP5A**: (a) 0.00 mM, (b) 0.16 mM, (c) 0.32 mM, (d) 0.48 mM, (e) 0.64 mM, (f) 0.80 mM, (g) 1.20 mM, (h) 1.60 mM, (i) 2.40 mM, (j) 3.20 mM, (k) 4.00 mM. Insert: The chemical shift changes of H-1 on FC_4 upon addition of **4C-WP5A**. The red solid line was obtained from the non-linear curve-fitting.

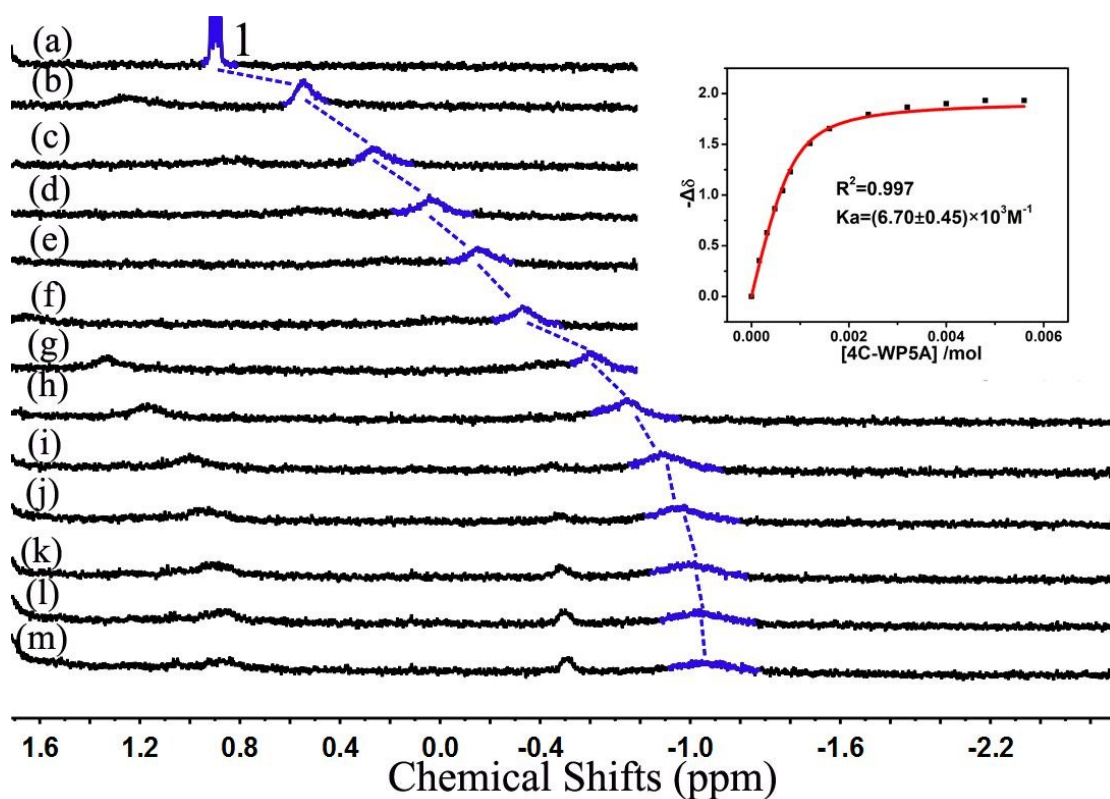


Figure S28. ^1H NMR spectra (D_2O , 293 K, 400 MHz) of FC_3^+ at a concentration of 0.8 mM upon different concentrations of **4C-WP5A**: (a) 0.00 mM, (b) 0.16 mM, (c) 0.32 mM, (d) 0.48 mM, (e) 0.64 mM, (f) 0.80 mM, (g) 1.20 mM, (h) 1.60 mM, (i) 2.40 mM, (j) 3.20 mM, (k) 4.00 mM, (l) 4.80 mM, (m) 5.60 mM. Insert: The chemical shift changes of H-1 on FC_3^+ upon addition of **4C-WP5A**. The red solid line was obtained from the non-linear curve-fitting.

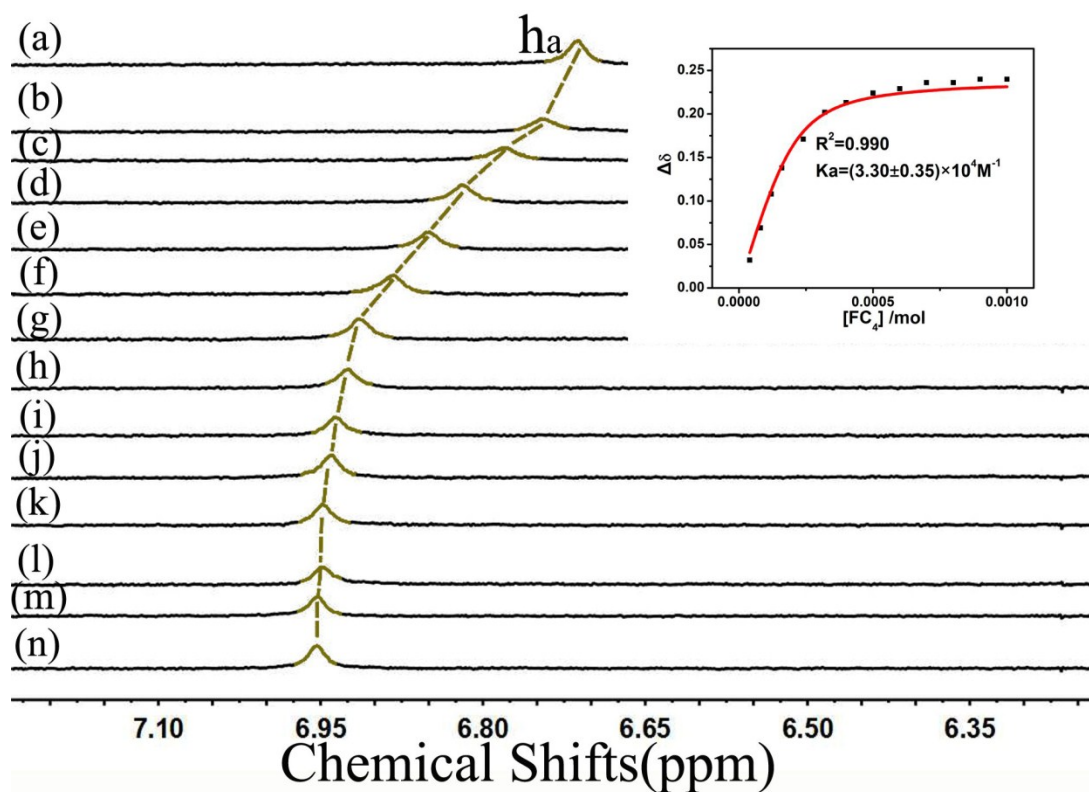


Figure S29. ¹H NMR spectra (D₂O, 293 K, 400 MHz) of **4C-WP5A** at a concentration of 0.2mM upon different concentrations of **FC₄**: (a) 0.00 mM, (b) 0.04 mM, (c) 0.08 mM, (d) 0.12 mM, (e) 0.16 mM, (f) 0.24 mM, (g) 0.32 mM, (h) 0.40 mM, (i) 0.50 mM, (j) 0.60 mM, (k) 0.70 mM, (l) 0.80 mM, (m) 0.90 Mm, (m) 1.00 mM Insert: The chemical shift changes of Ha on **4C-WP5A** upon addition of **FC₄**. The red solid line was obtained from the non-linear curve-fitting.

Table S1. Association constants (K_a) values and binding stoichiometry for inclusion complexations of G with host **4C-WP5A** in deuterium water at 298 K obtained by ^1H NMR titrations. The binding stoichiometry and the magnitude of K_a values are consistent with the ones measured by ITC.

Guest	Stoichiometry (H: G)	K_a
FC_1^+	1:2	— ^a
FC_3^+	1:1	$(6.70 \pm 0.45) \times 10^3$
FC_4^+	1:1	$(1.89 \pm 0.21) \times 10^4$
FC_4	1:1	$(3.30 \pm 0.35) \times 10^4$
FC_6^+	1:1	$(2.33 \pm 1.06) \times 10^5$
FC_8^+	1:1	$(3.18 \pm 1.41) \times 10^5$

a. For 2:1 complexes $4\text{C-WP5A} \supset \text{FC}_1^+$, the K_{av} values are very small and cannot be calculated accurately.

7. The investigations of the complexation for FC₁₈⁺ and 4C-WP5A

FC₁₈⁺ is a amphiphilic surfactant, which is easily dissolved in CH₂Cl₂ but not well dissolved in water. The ¹H NMR spectra in CDCl₃ and D₂O were shown as following:

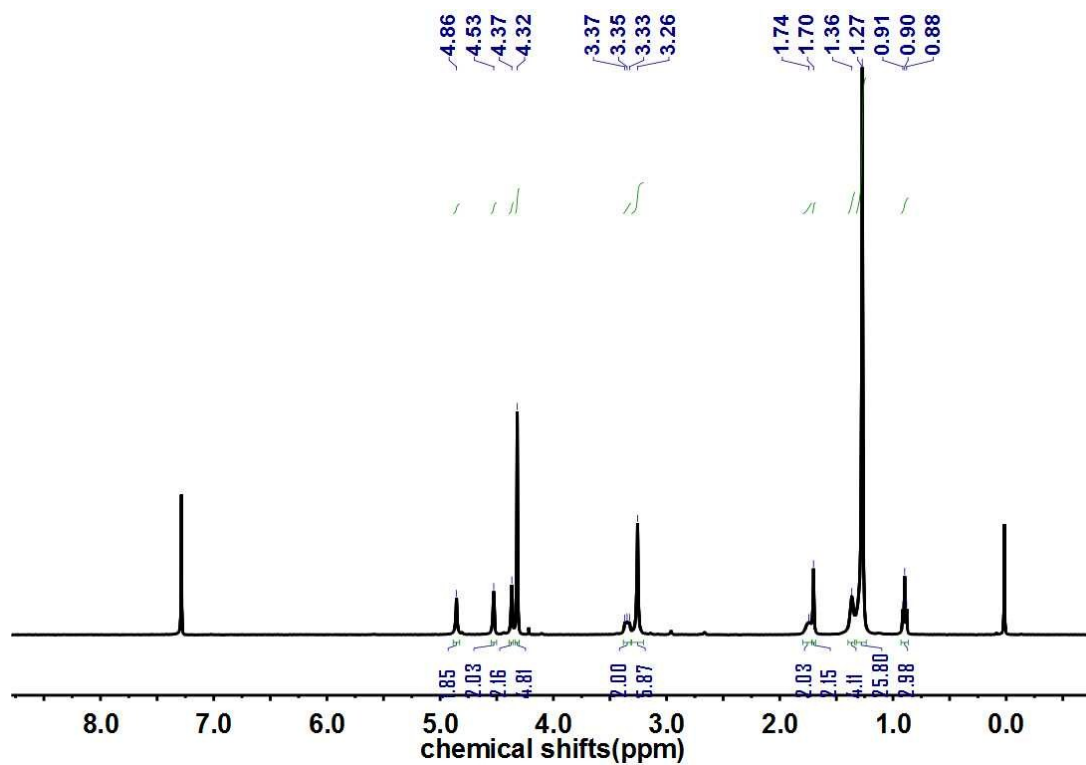


Figure S30. ¹H NMR spectrum (400 MHz, CDCl₃, 25 °C) of 5mM FC₁₈⁺.

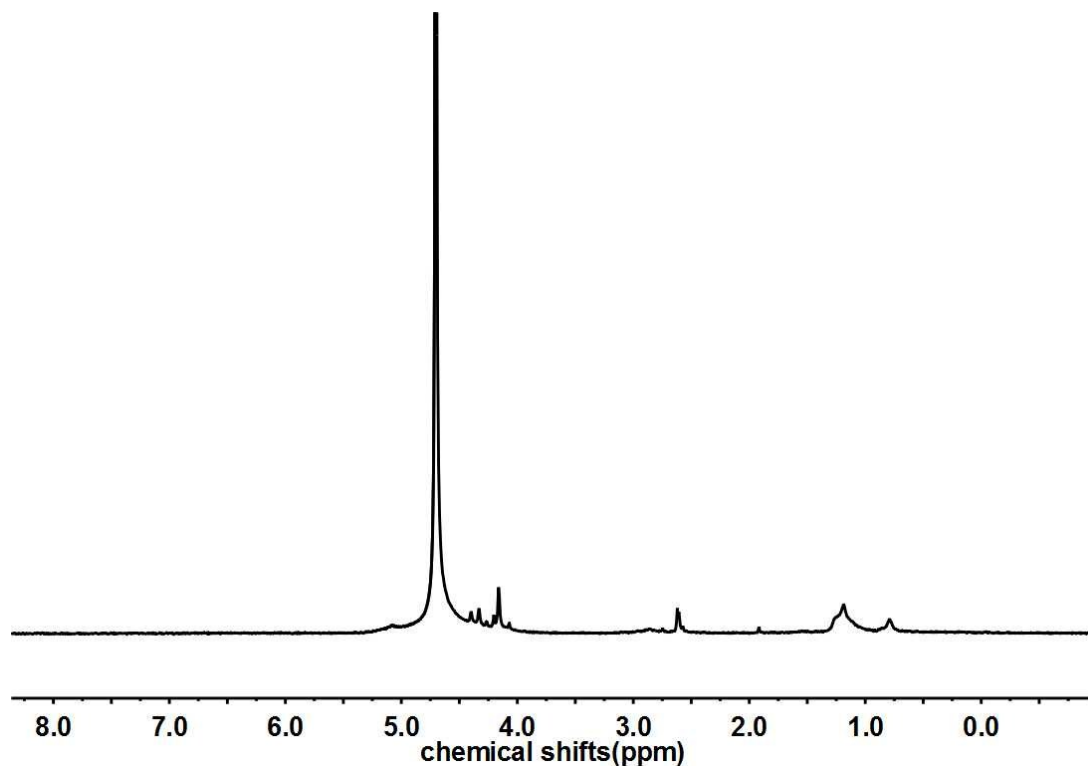


Figure S31. ^1H NMR spectrum (400 MHz, D_2O , 25 °C) of 0.4mM (the maximum solubility) FC_{18}^+ .

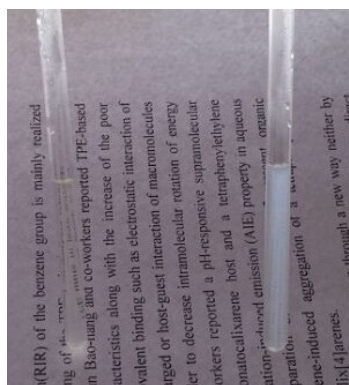


Figure S32. 0.4mM FC_{18}^+ (left) and 0.4mM FC_{18}^+ + 0.08mM **4C-WP5A** (right) in NMR tubes. According to literatures, the critical aggregation concentration of guest would be decreased in the presence of **WP5A**.^{S4,S5} Similarly, the obvious turbidity can be observed in our case, so it is difficult to study the binding behavior of **4C-WP5A** \supset FC_{18}^+ by ^1H NMR experiment.

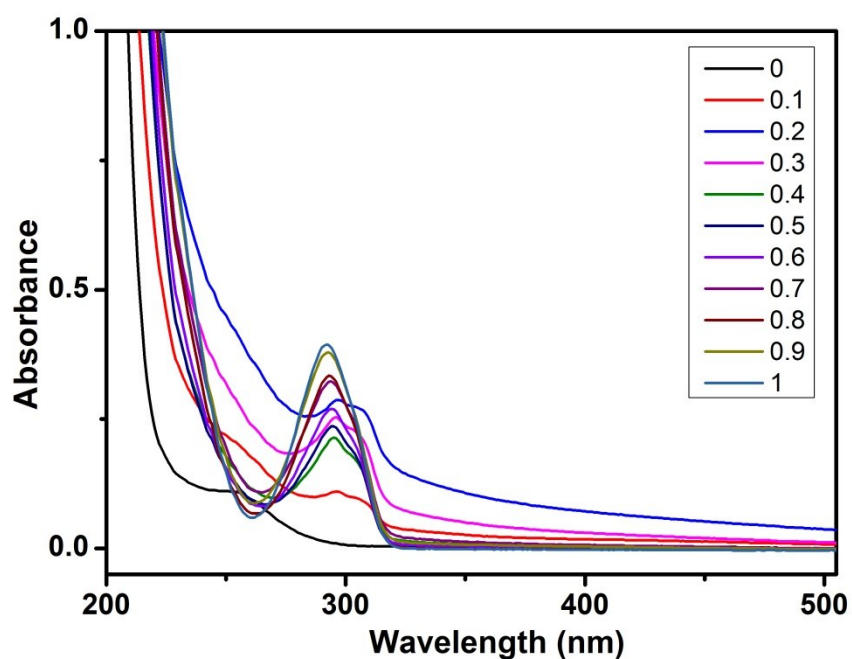


Figure S33. UV-Vis spectra ($[4\text{C-WP5A}] + [\text{FC}_{18}^+] = 25\mu\text{M}$) with the molar ratio of **4C-WP5A** is: 0, 0.1, 0.2, 0.3, 0.4, 0.5, 0.6, 0.7, 0.8, 0.9, 1.0. The lower transmittance in these UV-Vis spectra indicates that **4C-WP5A** and **FC₁₈⁺** were still aggregated at these dilute concentrations. So it is difficult to study the binding behavior because the interactions of **4C-WP5A** and **FC₁₈⁺** in water did not only include the molecular binding but also include the molecular self-assembly.

8. Reference

- S1. Z. Cheng, B. Ren, M. Gao, X. Liu and Z. Tong, *Macromolecules*, 2007, **40**, 7638–7643.
- S2. D. Pei, J. Hong, F. Lin, Z. Shi, Z. Chen, H. Nie, X. Guo, *Chem. Commun*, 2011, **47**, 9492–9494.
- S3. Y. Ma, X. Ji, F. Xiang, X. Chi, C. Han, J. He, Z. Abliz, W. Chen and F. Huang, *Chem. Commun*, 2011, **47**, 12340–12342.
- S4. G. Yu, X. Zhou, Z. Zhang, C. Han, Z. Mao, C. Gao and F. Huang, *J. Am. Chem. Soc.*, 2012, **134**, 19489–19497.
- S5. Y. Yao, X. Chi, Y. Zhou and F. Huang, *Chem. Sci.*, 2014, **5**, 2778–2782.